Department of Precision and Microsystems Engineering

Proposed solutions for quantization induced performance deterioration in reset controllers.

Bas Kieft

Report no : 2020.018
Coach : Dr. Niranjan Saikumar
Professor : Dr. Hassan HosseinNia
Specialisation : Mechatronic System Design
Type of report : MSc Thesis
Date : 03 June 2020

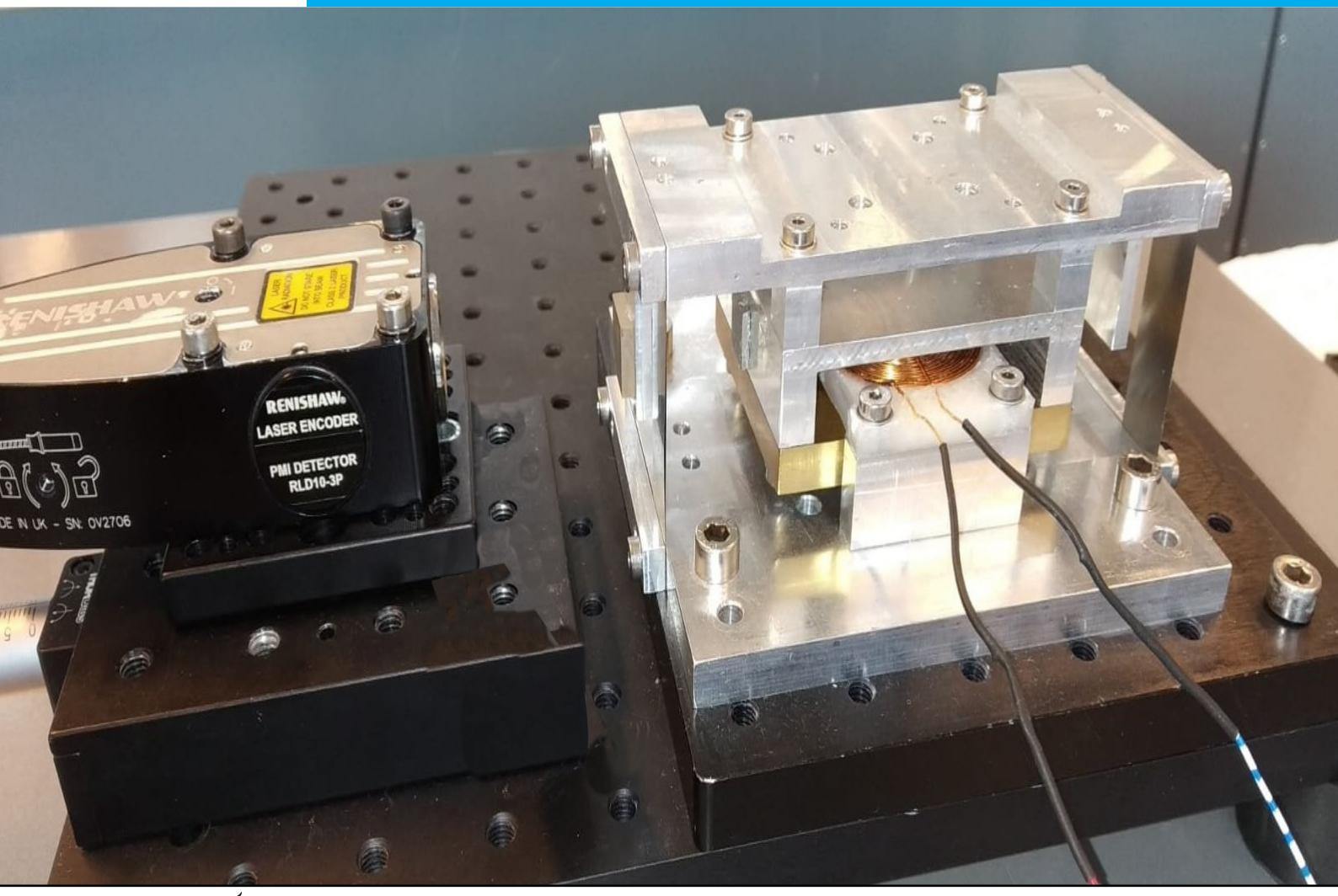

TU Delft Delft University of Technology

Precision and Microsystems Engineering

Challenge the future

Preface

First of all I would like to thank my supervisors; Niranjan Saikumar, Arnold Zondervan and Hassan Hosseinia. All have helped, challenged and motivated me in a variety of ways.

Arnold has supported me with the practical issues of the "Hittech" stage, a stage that was the primary validation unit. However, due to the circumstances of these times it was no longer possible to use this stage. Arnold helped me tremendously and with a quick meeting a take-home stage was put together. Unfortunately this stage turned out to be not suitable for the type of experiments that was required.

Niranjan and Hassan promptly stepped up and arranged a stage at the TU Delft Mechatronics lab. Here my colleagues where so flexible that I was able to perform the experiments in a short time. Especially Niranjan was able to help me with the practical matters of the TU Delft fine stage.

Niranjan has helped me in shaping the bones of my papers by supplying feedback throughout the year. For dotting the i's of my papers Hassan has put in some great effort in order to bring my writing to a more scientific level. Both Hassan and Niranjan have been tremendous co-authors for the papers.

I have always loved discussion about technical issues and all my supervisors where good sparring partners. My meetings with Arnold and Niranjan always supplied me with renewed interest, ideas or creativity. The "monday morning" meetings that were held at the TU Delft Precision and Microsystem Engineering (PME) square were another prime discussion platform. I enjoyed going there every week and either present or contribute to fellow colleagues. It, of course, had nothing to do with the free coffee that was supplied.

Although the conditions of the world today can be described as distant, isolated or removed, I can also state that there has been a lot of compassion, empathy and understanding.

Bas Kieft
Delft, June 2020

Abstract

The most widely applied feedback controller is PID. This controller gains its popularity because of the ease of design through *loop shaping*, since PID can be analyzed in the frequency domain. However, PID is limited by linearity.

Reset control is a nonlinear addition to PID control. *Through linearization techniques it can be designed by analyzing the frequency domain.* Through numerous numerical, analytical and practical experiments it has been shown that reset control can outperform PID.

However, when practically implementing reset control, especially in motion stages, one aspect can cause severe performance degradation. Research is underrepresented in this field. Quantization can be described as discretization in the amplitude. This thesis aims to reduce the quantization induced performance degradation. Two methods are proposed: reset band and time regularization.

Numerical analysis and practical experiments have been performed in order to analyze the performance degradation and proposed methods. Through the numerical analysis in matlab simulink of a mass system the performance degradation has clearly been addressed. Based on the new understanding tuning rules have been provided for both proposed methods. A preliminary sensitivity analysis shows the robustness of both methods.

Both proposed methods show enhanced performance. In numerical analysis it was shown that the reset band solution and time regularization can achieve an improvement of up to 10 dB.

It was shown through experiments on a high level motion stage that several dB improvement is feasible. For the reset band at a specifically detrimental frequency the error was reduced from 200 nm to 70 nm.

The reset band shows an improvement of several dB. In one setup, the performance enhancement spanned a wide frequency range.

Overall it is concluded that for quantization induced performance degradation both proposed methods clearly show improvement.

Two novel applications of existing methods have shown an increase in performance. New tuning guidelines have been provided.

Contents

1 Introduction

1.1. Introduction

Speed, precision and robustness are crucial factors at the forefront of mechatronic system design. For example, speed often relates directly to the throughput of a machine and is as such a prime factor in the revenue that a machine generates. Precision can be related to the quality of the product. For mechatronic system designers in the chip manufacturing business precision will dictate the value of the product **euv asml bron?**. Then there is robustness; robustness is crucial for maintaining stability in environments with all sorts of varying factors, such as temperature.

However, for the most commonly used feedback controller (PID) these imperative factors (speed, precision and robustness) are adverse. A limitation described by Bode as the gain-phase relationship is the cause of this trade off [4]. As a simplification one can say that the gain of a system relates to precision and speed, whereas phase is required for robustness and stability. PID owes its popularity to the ease of design that can be achieved by looking at the frequency domain. This loop shaping method has been refined with tuning rules that all control designers should know, often known as Rules of Thumb (ROT).

Reset control can be applied as a nonlinear supplement to PID. Through a linearization method known as the Sinusoidal Input Describing Function (SIDF) reset elements can be designed through the basis of loop shaping [7, 9]. Thanks to the inherent nonlinearity that is the resetting of an integrative element under certain conditions reset elements can circumvent Bodes gain-phase relationship. This allows reset controllers to outperform PID. For an example where it is analytically shown that reset can outperform PID see [3].

As an example, consider the first introduced reset element. The Clegg Integrator (CI) was introduced by Clegg in 1958 [7]. The CI resets the integrator state when the input of the element is zero, thus reducing the overshoot of a system. In feedback control the input of control elements is the error between the reference and the actual value. A standard integrator is known to have a so called -1 gain slope, which corresponds to a -90° phase as described by Bode's gain-phase relationship. Through a SIDF analysis it is shown that the CI achieves a -38.1° phase while maintaining the same gain slope. This enables the CI to have more robustness than a standard integrator, while maintaining the same speed and precision.

A plethora of reset elements have been designed. Among these are first and second order low pass filters (LPF). The First Order Reset Element (FORE) is a first order LPF with reset applied [11] and the Second Order Reset Element (SORE) is a second order LPF with reset applied [10]. There even exists a reset element with constant gain while the phase increases [20].

Reset elements have been applied in a wide variety of practical setups. A PI+CI element was applied to an industrial heat exchanger in [23]. Furthermore, this paper researches the application of a variety of reset conditions. A precision instrument where positioning speed is crucial for performance is a Hard Disk Drive (HDD). HDD have been used as a baseline for reset elements applied to motion control in [9, 14, 15]. Servo motors are present in many mechatronic systems, therefore [12] has done research into the application of

reset control in this field. Applications of reset control span the field from tape-speed setups [25] to exhaust gas re-circulation[17].

Even though the application of reset control on practical setups has been numerous, for example see [5, 6, 9, 12, 14–17, 21, 23], some practical issues have not extensively been addressed. One such a practical issue is the quantization that occurs in sensors or in the conversion from analogue to digital. Quantization has been researched in relation to reset control in [24], however the reset element was placed in the context of an observer.

Quantization can be described as a discretization in amplitude which results in a distorted signal [19]. This distorted signal in turns distorts the error. For reset elements, the error is an imperative value, for it is what initiates the resetting action under predetermined conditions. Therefore, the question arises whether quantization can cause problems and if so, how can we solve these?

In this thesis it has been shown through numerical and practical examples that quantization can cause performance degradation due to excessive resetting. This deterioration results in a decrease in the crucial factor of precision. Therefore this thesis endeavors to mitigate this performance degradation, such that the industrial core value of precision will be improved.

1.2. Problem definition

Quantization can cause performance deterioration for reset controllers, especially in situations where the error is small. In order to increase the effectiveness of reset control this performance deterioration needs to be resolved.

1.3. Research goal

The goal of this thesis is *to find solutions to mitigate quantization induced performance degradation.*

1.4. Thesis outline

The thesis is structured in a paper style with filler material.
Chapter 1 gives the introduction, problem definition, research goal and outline of this thesis. In Chapter 2 the preliminaries required for the context of the thesis are provided for. Two solutions are proposed in paper format: Chapter 3 proposes the reset band as a solution; and time regularization is proposed as a solution in Chapter 4. In Chapter 5 the combination of the two proposed solutions is considered as a possibility. Chapter 6 puts the experiments in perspective with PID control. A conclusion is given in Chapter 7 where also recommendations are made.

2

Preliminaries

In this chapter the preliminaries necessary to understand the thesis and included papers will be provided. If a more detailed and complete explanation is desired [22] is recommended.

2.1. Loop Shaping

Loop shaping is a method in which the controller is designed to get a desired shape in the gain and phase of the open loop transfer function (L(s) = Controller(s) ·Plant(s)).

See Fig. 2.1 for the definitions of signals where r is the reference, e is the error, u is the controller output (CO) or control input, d stands for disturbance, v is the total input of the plant, n is the noise, y' is the ideal sensor value and y is the sensor value. For motion systems y' will represent the true position of the stage.

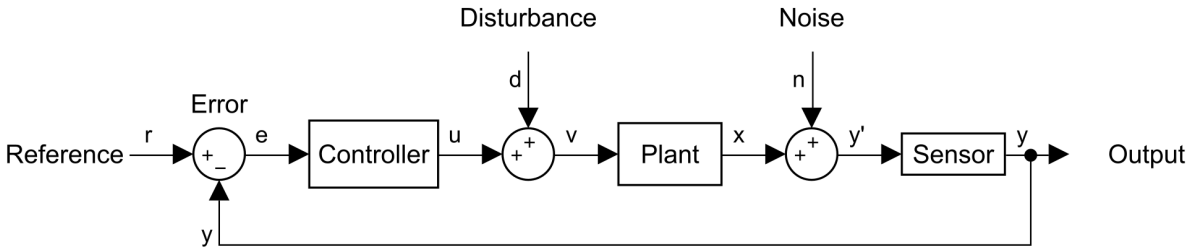

Figure 2.1: Block diagram definition.

2.1.1. Limitations of linear control

Three key components are adverse; speed, precision and robustness. In linear control theory a meaningful notion exists that is attributed to Bode [4] is known as *Bode's Phase-Gain relationship* or otherwise known as the *waterbed effect*. This notion revolves around the dynamic where when linearly adding phase to improve robustness, gain is added. This increased gain results in a decrease of precision.

2.2. Reset control

Reset control is based on a dynamic where an integrative element resets when its input is zero. The first reset element is the Clegg Integrator (CI) and was introduced in 1958 by J.C. Clegg [7]. Because the CI is a nonlinear element its dynamics are linearized through a Sinusoidal Input Describing Function (SIDF). When analyzing the SIDF of the CI it can be seen that its phase is -38° where the phase of the linear integrator is -90°. This decreased loss in phase is beneficial for the trade-off that was discussed prior.

A plethora of reset elements have been introduced that revolve around the CI. For example, an element known as the Constant in gain Lead in phase (CgLp) can add phase without changing gain and therefore breaks through the limitations of Bode's gain phase relationship [21]. Reset control can be categorized as an impulsive system [1]. For an overview of reset control [1] is recommended.

2.2.1. Reset Control Definition

In literature several definitions can be found referring to Reset Control. Zaccarian [18] shows some of these definitions. For this thesis the definition in line with [1] will be followed. This definition has been expanded upon such that it leads to the form seen in Equation 2.1, for example [21] and [9].

$$(R): \begin{cases} \dot{\mathbf{x}}_r(t) = A_r\mathbf{x}_r(t) + B_r e(t) & \text{if } e(t) \neq 0 \\ \mathbf{x}_r(t^+) = A_\rho \mathbf{x}_r(t) & \text{if } e(t) = 0 \\ u(t) = C_r\mathbf{x}_r(t) + D_r e(t) \end{cases} \tag{2.1}$$

Where $\mathbf{x}_r(t)$ are the reset states, $\dot{\mathbf{x}}_r(t)$ are the derivative of the reset states, $u(t)$ is the output of the reset controller and e is the error. t^+ signifies the instance just after reset. The first line of Equation 2.1 is referred to as the flow state, whereas the second line is known as the jump state. A_ρ is diagonal and is the reset matrix that determines the states to be reset. For a full reset A_ρ is the zero matrix and for a linear controller this is the identity matrix.

2.2.2. Describing Function

Reset Control is non-linear and is as such not directly useable in the frequency domain. Therefore a Sinusoidal Input Describing Function (SIDF) analysis is to be performed such that the reset control element is approximated. The derivation of a DF for the system of Equation 2.1 with a sinusoidal input is given in [9]. Equation 2.2 is the describing function. This is in the form of the transfer function $G(j\omega) = \frac{Yss(j\omega)}{E(j\omega)}$.

$$G(j\omega) = C_r^T(j\omega I - A_r)^{-1}(I + j\Theta_\rho(\omega))B_r + D_r \tag{2.2}$$

where

$$\Theta_\rho \triangleq \frac{2}{\pi}\left(I + e^{\frac{\pi A_r}{\omega}}\right)\left(\frac{I - A_\rho}{I + A_\rho e^{\frac{\pi A_r}{\omega}}}\right)\left(\left(\frac{A_r}{\omega}\right)^2 + I\right)^{-1}.$$

2.2.3. Stability

Closed loop stability can be checked by the H_β-condition [1]. To analyse closed loop stability the closed loop reset control definition from [1] is followed.

Of the closed loop system with dimension $n = n_p + n_r$, where n_r signifies the number of states being reset and the subscript p for the elements denote that these are for the plant, the state can be described as:

$$\mathbf{x} = \begin{bmatrix} \mathbf{x}_p \\ \mathbf{x}_r \end{bmatrix},$$

The closed loop system is then:

$$\begin{cases} \dot{\mathbf{x}}(t) = A_{cl}\mathbf{x}(t) & \text{if } e(t) \neq 0 \\ \mathbf{x}(t^+) = A_R\mathbf{x}(t) & \text{if } e(t) = 0 \end{cases}$$

where

$$A_{cl} = \begin{bmatrix} A_p & B_pC_r \\ -B_rC_p & A_r \end{bmatrix}$$

and

$$A_R = diag(I_{np}, A_\rho)$$

A_{cl} denotes the closed loop A-matrix.

Closed loop stability can be checked by the H_β-condition. For a reset controller defined as Equation 2.1 the system is quadratically stable if there exists a $\beta \in \mathbb{R}^{n_p \times 1}$ and a positive definite $P_\rho \in \mathbb{R}^{n_r \times n_r}$ such that the restricted Lyapunov Equation (2.3, 2.4) has a solution for P.

$$P > 0, \quad A_{cl}^T P + P A_{cl} < 0 \tag{2.3}$$

$$B_0^T P = C_0 \tag{2.4}$$

where

$$C_0 = \begin{bmatrix} \beta C_p & 0_{n_r \times n_{nr}} & P_\rho \end{bmatrix}, B_0 = \begin{bmatrix} 0_{n_p \times n_{nr}} \\ 0_{n_{nr} \times n_r} \\ I_{nr} \end{bmatrix}.$$

An equivalent condition is known as the H_β-condition, given in Equation 2.5. Equivalency is shown in [1].

There exists a positive-definite matrix $P_\rho \in \mathbb{R}^{n_\rho \times n_\rho}$ and $\beta \in \mathbb{R}^{n_\rho \times 1}$ such that

$$H_\beta(s) := C_0(sI - A)^{-1}B_0 \tag{2.5}$$

is a strictly positive real (SPR) transfer function, where (A,B_0) is controllable and (A,C_0) is observable.

2.2.4. Reset Elements

Reset Control is based on the resetting of the integrator term. The instantaneous disposal of the redundant integrator output results in a reduced phase lag. Multiple types of Reset elements can be found in literature, several of these will be emphasized in this section.

Clegg Integrator

The most simple and classical example of a Reset Controller is the aforementioned Clegg Integrator (CI). Following the definition of Equation 2.1 the CI is defined as $A_r = 0$, $B_r = 1$, $C_r = 1$, $D_r = 0$ and $A_\rho = 0$. When plotting the CI and the first order DF of the CI a clear difference is visible. See Figure 2.2a for the time response for a sinusoidal input with $u(t) = sin(2t)$. When looking at Figure 2.2b it can be seen that for the 2 rad/s input the integrator has a gain of $\frac{1}{2}$ and the CI has a gain of 0.81. When checking Clegg's work [7] it can be seen that the CI has a gain of 1.62 times a linear integrator.

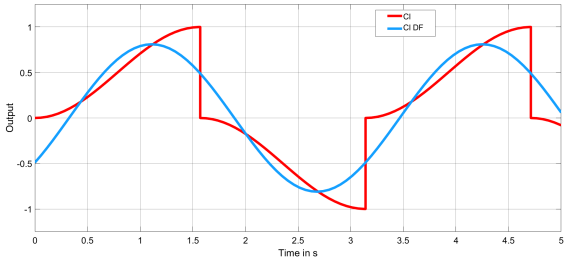

(a) Clegg integrator and it's SIDF in the time domain for $u(t) = sin(2t)$.

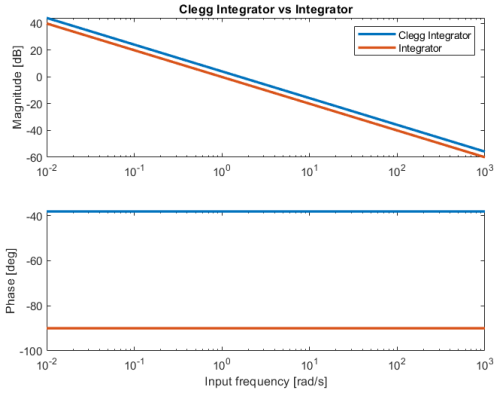

(b) Clegg integrator and a normal integrator in the frequency domain.

Figure 2.2: Analysis of a Clegg integrator.

FORE

Horowitz has introduced a First Order Reset Element (FORE) [11]. The FORE can also be seen as a non-linear low-pass filter (LPF) with corner frequency ω_r. Following the definition of Equation 2.1 the FORE is defined as $A_r = -\omega_r$, $B_r = \omega_r$, $C_r = 1$, $D_r = 0$ and $A_\rho = 0$. A generalisation for FORE (GFORE) has been defined in [9] where $A_\rho = \gamma$ in which $-1 \leq \gamma \leq 1$ makes GFORE a partial reset element. A base linear low-pass filter is represented by $\gamma = 1$. Figure 2.3 shows the phase lag reduction of FORE over a linear low-pass filter in a bode plot.

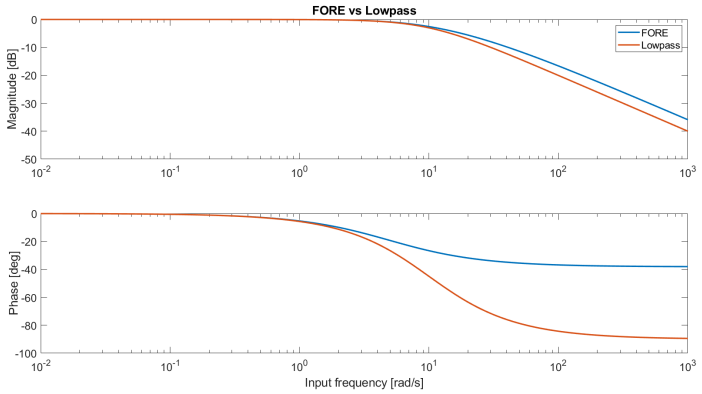

Figure 2.3: FORE and a linear low-pass filter in the frequency domain.

SORE
FORE has been expanded upon to introduce a Second Order Reset Element (SORE) [10]. They particularly studied the second-order low-pass filter, though it was noted that a notch filter could also be possible. SORE has been defined according to Equation 2.1 with the following matrices:

$$A_r = \begin{bmatrix} 0 & 1 \\ -\omega_r^2 & -2\beta_r\omega_r \end{bmatrix}, B_r = \begin{bmatrix} 0 \\ \omega_r^2 \end{bmatrix},$$

$$C_r = \begin{bmatrix} 1 & 0 \end{bmatrix}, D_r = \begin{bmatrix} 0 \end{bmatrix}.$$

where β_r is the dampening coefficient. As with GFORE also SORE has been generalized to include partial reset with a non-zero reset matrix. In [21] the effects of generalizing SORE (GSORE) are shown.

Constant in Gain Lead in Phase
Constant in Gain Lead in Phase (CgLp) is a more recent element which essentially combines GFORE with a linear lead filter or combines GSORE with a linear second order lead filter [21]. In fully linear control the gains and phases of the LPF and Lead would cancel out. However, because the GFORE has a phase lag of only 38° the total phase will be approximately 52° lead while the gain remains roughly canceled. This enables the controller to add phase lead for a certain frequency domain. The state space of the first order CgLp is defined according to Equation 2.1 with:

$$A_r = \begin{bmatrix} -\omega_{r\alpha} & 0 \\ \omega_f & -\omega_f \end{bmatrix}, B_r = \begin{bmatrix} \omega_{r\alpha} \\ 0 \end{bmatrix},$$

$$C_r = \begin{bmatrix} \frac{\omega_f}{\omega_r} & (1 - \frac{\omega_f}{\omega_r}) \end{bmatrix}, D_r = \begin{bmatrix} 0 \end{bmatrix},$$

$$A_\rho = \begin{bmatrix} \gamma & 0 \\ 0 & 1 \end{bmatrix}.$$

Where $\omega_{r\alpha}$, ω_f and ω_r are the corner frequencies for the FORE, linear LPF and linear Lead respectively. An example of the benefits of CgLp is shown in Figure 2.4 where a phase lead of 20° was achieved while maintaining a constant gain for a range of one decade.

Alternatively the CgLp can be defined in the frequency domain as:

$$\frac{1}{\cancel{s/\omega_{r\alpha} + 1}} \gamma \frac{s/\omega_r + 1}{s/\omega_f + 1}.$$

2.2.5. CgLp-PID

CgLp-PID is a CgLp element combined with a linear PID controller, in this thesis the choice was made to follow the CgLp · PID order. The order of elements is important because the CgLp-PID includes a non-linear element. In [5] an analysis has been performed into the order of resetting. The design procedure for CgLp-PID is stated in [21]. It is required to have a stable base linear system.

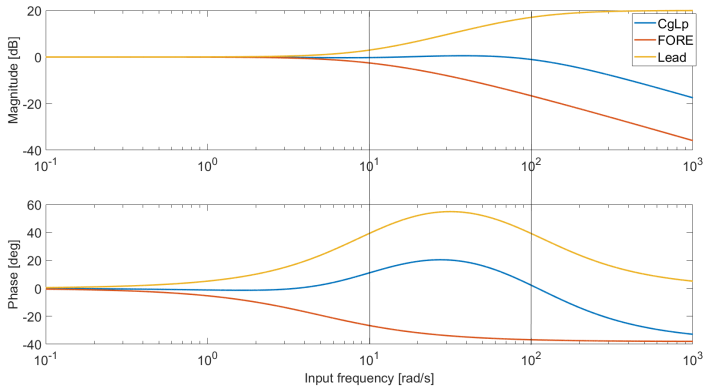

Figure 2.4: CgLp, FORE and Lead in the frequency domain for $[\omega_r, \omega_f, \alpha]$ = [10, 100, 1.2].

CgLp, having the constant gain but lead in phase, can be used to partially or completely replace the D part of PID. A CgLp-PID can be represented as:

$$\underbrace{P(1+\frac{\omega_i}{s})}_{PI}\underbrace{\frac{(s/\omega_d+1)}{(s/\omega_t+1)}}_{D}\underbrace{\frac{1}{s/\omega_{r\alpha}+1}\gamma\frac{s/\omega_r+1}{s/\omega_f+1}}_{CgLp} \tag{2.6}$$

The phase lead provided by D can be tuned by varying a in $\omega_d = \omega_c/a$ and $\omega_t = \omega_c a$. The phase lead provided by CgLp can be tuned by ω_r and γ. With sufficiently small ω_r and $\gamma = 0$ it is possible to provide 52° phase lead.

Others
There are still other approaches to reset control, some fundamentally differ. When talking about a standard reset, the reset condition condition $e = 0$ is meant. However, there are other reset conditions such as a fixed or variable reset band where the system will be reset if the error enters a band [1, 2].
Another method is fixed-time reset [14] which could also be assigned in a different impulsive system class [1].

2.3. Quantization

Quantization can be described as discretization in the magnitude. Its causes can be both analog or digital. Figure 2.5 shows the effect of quantization. Quantization can be recognized that for example a ramp input results in a staircase output.

2.3.1. Quantization introduction

The error that is associated with quantization is known as distortion $(y' - y)$. This is shown in red in Figure 2.5. For a ramp, distortion will look like a saw-tooth profile. Quantization can be handled in multiple ways, for example dynamic versus static, linear versus logarithmic. In this thesis the common static linear quantization will be applied, because most encoders have physical static, linear quantization. There are two types of static, linear quantization: rounding and truncation [19]. Due to its abundance in industry the latter will be standard in this thesis. As can be seen in Figure 2.5, the difference between the two methods is that for rounding quantization the true error $(r - y')$ is in the middle of quantization jumps of $(r - y)$. For truncation quantization the sensed error is touching the lower end of the true error. However, since a controller controls for y and has no information about the true error the response will be (near) identical for both types of quantization. This will be further explained after a small preliminary about quantization.

For digital quantization a quantization level is defined as $Q = \frac{Range}{2^{bits}}$. Range can be described as the biggest value that can be detected. Bits is related to the digitization of the data and represents the number of bits available to show the magnitude of the value. For example, for a sensor with a range of $1000nm$, several digitization processors are available, 5 bit and 6 bit. The 5 bit and 6 bit systems will result in a resolution of $\frac{1000nm}{2^5} = 31.25nm$ and $\frac{1000nm}{2^6} = 15.63nm$ respectively. The boundary between two Q's can be referred to as a

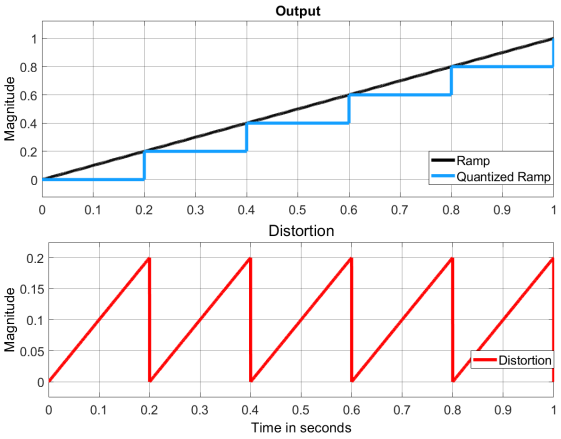

(a) Truncation quantization and distortion for Ramp=t and Q=0.2.

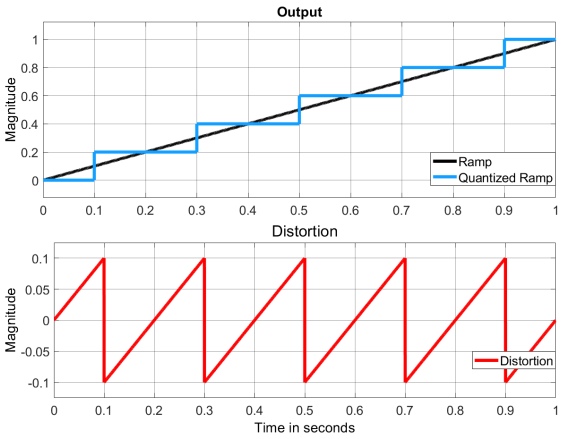

(b) Rounding quantization and distortion for Ramp=t and Q=0.2.

Figure 2.5: Truncation and rounding quantization.

jump or transition level.

Consider a PID controlled mass plant with a sufficiently high crossover frequency and a truncation quantization sensor. In Figure 2.6a the response of such a system is shown. For a ramp input, the error will be positive at the second time instance. Thus the controller will start to push the plant to the reference. However, until the true position of the plant passes a Q level no quantization jump is initiated, thus the distorted error will remain positive. As soon as the first Q is reached by the plant (Figure 2.6a: time≈0.04s, where the blue line crosses the green line), the distorted error jumps to a negative value because the quantized signal passes the reference (Figure 2.6a: the orange line passes the red line). Therefore the controller output will change direction and pull the plant back. This induces a backward quantization jump (when the blue line passes the green line with a downward slope) which causes the controller to push the plant up. This behavior is a *limit cycle* [8, 13] where the true position oscillates around a quantization jump level. This is true for both linear and non-linear controllers. This limit cycle will oscillate around a quantization jump point, rise time and overshoot determine the frequency and magnitude of the oscillation for it is a sequence of step responses. The difference in quantization jump points for truncation and rounding quantization is by definition $\frac{Q}{2}$. When the reference is bigger than Q the limit cycle will switch to the next Q. This can be seen in Figure 2.6a.

There is one significant difference in the response for truncation and rounding quantization. At the initial jump instance the magnitude of the jump depends on the type of quantization. For truncation quantization and for rounding quantization the jump will be of magnitude Q and $\frac{Q}{2}$ respectively. This difference in the magnitude of the jump in the error causes a difference in overshoot.

In Figure 2.6b the distortion and true error of the two types of quantization are compared. In black the difference in true error is shown. It can be estimated from the frequency of quantization jumps that the system in Figure 2.6b has a faster rise time than Figure 2.6a.

This leads to a remark that indicates that a solution for one type of quantization will work for the other as well:

Remark 1 *The distorted error behavior for truncation and rounding quantization is near identical.*

Literature often makes the statement that distortion can be modeled as white noise or as colored noise [26]. While this may be sufficient for implementing linear filtering techniques, it will not suffice here. The frequency of distortion is related to the slope of the ideal signal, the magnitude of Q and $C \cdot P$ dynamics. A gentle slope will cause a much lower distortion frequency compared to a steep slope. This is because a steep slope will cover more Q's for the same duration, and thus have much more closely sequenced saw-tooth profile. Figures 2.6a and 2.6b show two different distortion frequencies for two different controllers.

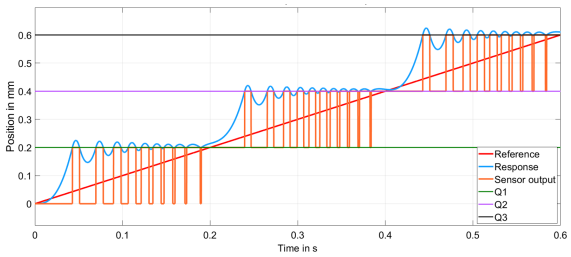

(a) PID controlled mass plant with truncation quantization.

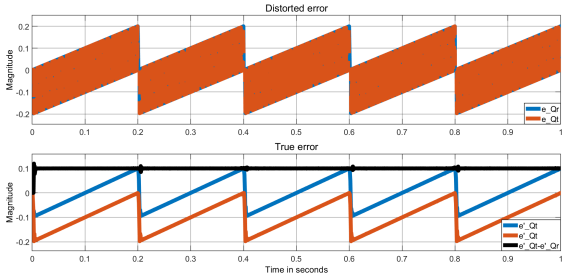

(b) Error of a PID controlled mass plant. Qr and Qt denote rounding and truncation quantization respectively.

Figure 2.6: Two PID controlled mass plants.

Quantization is relevant for reset control especially because the input of the reset condition is the error of the system. A distortion of this error will impact the behavior of the reset controller, specifically the instances and amounts of resets.

2.3.2. Quantization induced performance deterioration

On the one hand there is the reset controller which derives all its benefits from correctly resetting based on its input, which is the error. On the other hand there is a distortion of the error due to quantization. This distortion can cause pseudo zero error crossings where in reality there was no crossing. In other words, y crosses the reference where y' does not. The other way around where crossings are missed is also possible, y' crosses the reference where y does not. Especially the pseudo zero error crossings can induce problematic behavior and thus cause performance deterioration.

Figure 2.7 shows an example of numerical and simulated performance deterioration in Figures 2.7a and 2.7c [1]. The start of the deterioration cycles are shown in Figures 2.7b and 2.7d. These examples are for CgLp-PID controllers with motion systems.

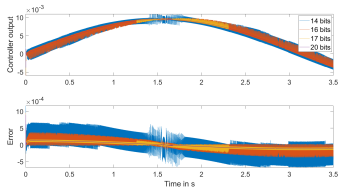

(a) Numerically shown performance deterioration for a range of Q.

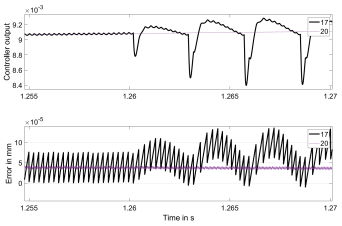

(b) Numerically shown start of performance deterioration for two Q's.

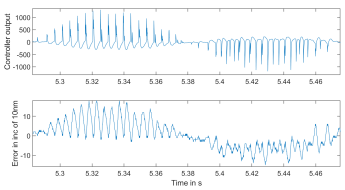

(c) Experimentally shown performance deterioration.

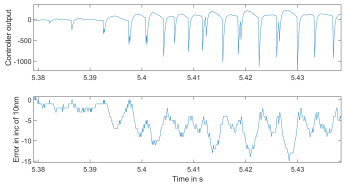

(d) Experimentally shown start of performance deterioration.

Figure 2.7: Set of performance deterioration for CgLp-PID controllers for mass-spring-damper plants.

[1] The controller output plotted is negative because of an inversion in the power amplifier.

3

Reset Band

This chapter is in in paper format. The paper proposes a reset band as a solution for quantization induced performance degradation. The paper is planned to be submitted to the 2021 European Control Conference (ecc21).

3.1. Reset band paper

Reset band as a solution to mitigate quantization induced performance degradation

Bas Kieft, Niranjan Saikumar, and S. Hassan HosseinNia *Senior Member, IEEE*

***Abstract*—Reset control is known to be able to outperform PID. However, for motion control systems quantization can cause severe performance degradation. This paper repurposed the reset band condition in order to mitigate said performance degradation. Novel tuning guidelines are provided for estimating the required reset band parameter.**

Numerical simulations have been conducted in matlab simulink on a mass system in order to analyze the cause of the quantization induced performance degradation. Moreover a performance and robustness analysis was performed. Experiments have been conducted on a high level motion system for validation.

The experiments show by example that the reset band can reduce the error in a problematic region from 200 nm to 70 nm for a high tech motion stage.

Our study reveals that the application of a reset band can significantly reduce quantization induced performance degradation.

***Index Terms*—Reset Control, Reset Band, Mechatronics, Motion Control, Implementation, Quantization.**

I. Introduction

RESET control has gained popularity because it enables controller design that overcomes the limitations of linear control as posed by Bode [1]. Reset control is a nonlinear alteration of PID control that reduces the decoupling of gain and phase characteristics, thus diminishing Bode's limitation.

Clegg first introduced reset with a Clegg Integrator (CI) [2]. This element is an integrator where the state is reset to zero when the input is zero. This reduces phase lag from -90° to -38°. In continuation of reset control the First Order Reset Element (FORE) was created [3]. The Second Order Reset Element (SORE) [4] is the natural advancement of the FORE. In [5] a CI with fractional order is studied, thereby increasing the freedom of tuning farther.

A different take on tunable nonlinearity is applied in hybrid control and partial reset. For these systems the after reset value is tunable. Hybrid control [6] where a CI and I work in parallel and is also known as PI+CI. Another approach is partial reset, where the state of the integrator is not reset to zero but to a predetermined fraction of the gain at the time of reset. This lead to the Generalized FORE (GFORE) [7] and the Generalized SORE (GSORE) [8].

Reset control has a lot of theoretical benefits. Therefore it is not unexpected that it has been applied in process industry and motion control. In [9] a PI+CI element was applied to an industrial heat exchanger. Moreover, in this paper a variety of reset conditions are applied and researched. Hard Disk Drive (HDD) are precision motion instruments where positioning speed is crucial for performance. Therefore a research group has used HDD as a base for reset control research [10], [11], [7]. Servo motors are the core of many motion control applications, so research into reset control application is imperative [5]. The applications of reset control are as diverse as a tape-speed setup [12] and exhaust gas re-circulation [13].

In the above stated applications reset control has been used to decrease phase lag introduced by an integrator. However, the decoupling of phase and gain allows for more interesting elements. The Constant in gain Lead in phase (CgLp) is a prime example of the possibilities [8], [14]. CgLp combined GFORE with a linear lead element and achieved what the name implies. This allows for a lowered dependency on the differential term.

Industry uses the frequency domain to model and tune the system. The frequency domain approach is based on linear systems. With the introduction of the CI, Clegg used a Sinusoidal Input Describing Function (SIDF) to linearize this reset element. This approach was adopted for all discussed elements [2], [3], [4], [5], [6], [7], [8], [14].

In almost all cases in literature, results are extracted from simulations where generally continuous time implementations are used. In [15], [16], [8] the controllers were discretized. In most cases the steps associated with practical implementation do not cause issues. However, quantization is a type of practical issue that is not studied.

Quantization is a relevant signal disturbance that has been compared to noise. It has been researched extensively, e.g. [17], [18], [19]. Moreover, it's influence on linear control is well known [20], [21], [22]. In linear control quantization causes some mild limit cycling between quantization levels. Industry often prescribes the required resolution based on a safety factor times the desired precision. However, the research on the effect of quantization on reset control is lacking. Quantization with reset control is studied in [23], but only the application of reset control in the state estimator in order to mitigate quantization noise, known as distortion. For most reset control applications the reset condition is a zero error crossing, therefore any distortion in the error can cause improper resets or missed resets. This could lead to performance degradation. Although quantization is generally modeled as white or colored noise [24] this does not represent reality. For example, the frequency of distortion is dependent on the quantizer resolution and response slope.

If quantization is not considered reset control can outperform PID. However, quantization can cause performance degradation at lower frequencies for reset systems, while the benefit from reset systems is especially desired at frequencies around the bandwith. Therefore the desire arises to have a linear controller at lower frequencies and a reset controller at higher frequencies.

This paper studies the use of reset bands to achieve this split. Instead of a reset at the zero error crossing, the reset band method places a band around the zero error [25], [26]. In this approach reset occurs when entering this band. The application of this reset condition is not widely studied besides the work done by the original authors. No real tuning rules exist for this reset condition.

The main contributions of this paper are a proposed solution for quantization induced performance degradation based on the application of a reset band in order to split the controller in a linear and reset controller based on input frequency. Moreover, a method to tune the proposed solution and a describing function analysis with the inclusion of a reset band are provided.

The paper is structured as follows: Section II states the preliminaries required for the paper. Then in section III the performance degradation is expanded upon. A solution against the degraded performance is proposed in section IV. The results are validated in section V and the conclusion is given in section VI.

II. Preliminaries

A. Reset Control Definition

In literature several definitions can be found referring to Reset Control. Zaccarian [27] shows some of these definitions. For this research paper the definition in line with [26] will be followed. This definition has been expanded upon such that it leads to the form seen in Equation 1, e.g. [8] and [7].

$$(R): \begin{cases} \dot{\mathbf{x}}_r(t) = A_r\mathbf{x}_r(t) + B_r e(t) & \text{if } e(t) \neq 0 \\ \mathbf{x}_r(t^+) = A_\rho \mathbf{x}_r(t) & \text{if } e(t) = 0 \\ u(t) = C_r\mathbf{x}_r(t) + D_r e(t) \end{cases} \quad (1)$$

where $\mathbf{x}_r(t)$ are the reset states, $u(t)$ is the output of the reset controller and A_r, B_r, C_r and D_r are the state space matrices and are referred to as the base linear system. The first line of Equation 1 is referred to as the flow state, whereas the second line is known as the jump state. A_ρ is diagonal and is the reset matrix that determines the states to be reset and their after reset value. For a full reset A_ρ is the zero matrix and for a linear controller, this is the identity matrix.

B. Describing Function

Reset control is non-linear. Therefore a Sinusoidal Input Describing Function (SIDF) analysis is to be performed such that the reset control element is approximated. In [7] the describing function for the reset element of Equation 1 is presented:

$$G(j\omega) = C_r^T(j\omega I - A_r)^{-1}(I + j\Theta_\rho(\omega))B_r + D_r \quad (2)$$

where

$$\Theta_\rho \triangleq \frac{2}{\pi}\left(I + e^{\frac{\pi A_r}{\omega}}\right)\left(\frac{I - A_\rho}{I + A_\rho e^{\frac{\pi A_r}{\omega}}}\right)\left(\left(\frac{A_r}{\omega}\right)^2 + I\right)^{-1} \quad (3)$$

C. Stability

To analyse closed loop stability the closed loop reset control definition from [26] is followed.

Of the closed loop system with dimension $n = n_p + n_r$ where n_r signifies the number of states being reset and the subscript p for the elements denote that these are for the plant the state can be described as:

$$\mathbf{x} = \begin{bmatrix} \mathbf{x}_p \\ \mathbf{x}_r \end{bmatrix},$$

The closed loop system is then:

$$\begin{cases} \dot{\mathbf{x}}(t) = A_{cl}\mathbf{x}(t) & \text{if } e(t) \neq 0 \\ \mathbf{x}(t^+) = A_R\mathbf{x}(t) & \text{if } e(t) = 0 \end{cases}$$

where

$$A_{cl} = \begin{bmatrix} A_p & B_pC_r \\ -B_rC_p & A_r \end{bmatrix}$$

and

$$A_R = diag(I_{np}, A_\rho)$$

A_{cl} denotes the closed loop A-matrix.

Closed loop stability can be checked by the H_β-condition. For a reset controller defined as Equation 1 the system is quadratically stable if there exists a constant $\beta \in \mathbb{R}^{n_p \times 1}$ and a positive definite $P_\rho \in \mathbb{R}^{n_r \times n_r}$ such that the restricted Lyapunov Equation (4, 5) has a solution for P.

$$P > 0, \quad A_{cl}^T P + P A_{cl} < 0 \quad (4)$$

$$B_0^T P = C_0 \quad (5)$$

where

$$C_0 = \begin{bmatrix} \beta C_p & 0_{n_r \times n_{nr}} & P_\rho \end{bmatrix}, B_0 = \begin{bmatrix} 0_{n_p \times n_{nr}} \\ 0_{n_{nr} \times n_r} \\ I_{nr} \end{bmatrix}$$

and n_{nr} stands for the number of non-resetting states.

D. Reset Elements

1) Clegg integrator: Following the definition of Equation 1 the CI is defined as $A_r = 0$, $B_r = 1$, $C_r = 1$, $D_r = 0$ and $A_\rho = 0$.

2) FORE: Horowitz introduced a First Order Reset Element (FORE) [3] to allow for a nonlinear (reset) low-pass filter (LPF) with corner frequency ω_r. Following the definition of Equation 1 the FORE is defined as $A_r = -\omega_r$, $B_r = \omega_r$, $C_r = 1$, $D_r = 0$ and $A_\rho = 0$. A generalisation for FORE (GFORE) has been defined in [7] where $A_\rho = \gamma$ with $-1 \leq \gamma \leq 1$ makes GFORE a partial reset element. $\gamma = 1$ represents a base linear low-pass filter.

3) SORE: The Second Order Reset Element (SORE) was introduced in [4]. SORE has been defined according to Equation 1 with the following matrices:

$$A_r = \begin{bmatrix} 0 & 1 \\ -\omega_r^2 & -2\beta_r\omega_r \end{bmatrix}, B_r = \begin{bmatrix} 0 \\ \omega_r^2 \end{bmatrix},$$
$$C_r = \begin{bmatrix} 1 & 0 \end{bmatrix}, D_r = \begin{bmatrix} 0 \end{bmatrix}.$$

where β_r is the damping coefficient.As with GFORE also SORE has been generalized to include partial reset with a non-zero reset matrix [8].

4) Constant in gain Lead in phase element: The reset element used in this paper is the first order Constant in gain Lead in phase (CgLp) element [8], [14]. This element is build by combining a FORE element with a linear lead. A second order CgLp is possible by combining a SORE with a second order linear lead.

$$A_r = \begin{bmatrix} -\omega_{r\alpha} & 0 \\ \omega_f & -\omega_f \end{bmatrix}, B_r = \begin{bmatrix} \omega_{r\alpha} \\ 0 \end{bmatrix},$$
$$C_r = \begin{bmatrix} \frac{\omega_f}{\omega_r} & (1 - \frac{\omega_f}{\omega_r}) \end{bmatrix}, D_r = \begin{bmatrix} 0 \end{bmatrix},$$
$$A_\rho = \begin{bmatrix} \gamma & 0 \\ 0 & 1 \end{bmatrix}.$$

where $\omega_{r\alpha}$, ω_f and ω_r are the corner frequencies for the FORE, linear LPF and linear lead respectively.

E. CgLp-PID

The aforementioned CgLp element is best used in tandem with a PID controller. The CgLp-PID is a CgLp element multiplied with a linear PID controller, in this paper the choice was made to follow the CgLp *cdot* PID order. The design procedure is stated in [8]. It is required to have a stable base linear system.

CgLp, having the constant gain but lead in phase, can be used to partially or completely replace the D part of PID. A CgLp-PID can be represented as:

$$\underbrace{P(1 + \frac{\omega_i}{s})}_{PI} \underbrace{\frac{(s/\omega_d + 1)}{(s/\omega_t + 1)}}_{D} \underbrace{\frac{1}{s/\omega_{r\alpha} + 1}^{\gamma} \frac{s/\omega_r + 1}{s/\omega_f + 1}}_{CgLp} \quad (6)$$

The phase lead provided by D can be tuned by changing a in $\omega_d = \omega_c/a$ and $\omega_t = \omega_c a$. The phase lead provided by CgLp can be tuned by ω_r and γ. With sufficiently small ω_r and $\gamma = 0$ it is possible to provide 52° phase lead.

III. Quantization induced performance deterioration

1) Block diagram: the block diagram of control to be studied in this paper is shown in Fig. 1.

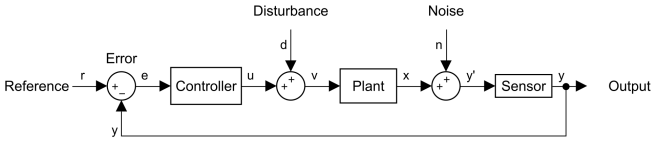

Fig. 1: Block diagram definition.

TABLE I: Controller settings applied to the mass stage.

P	6.0954e+05	-
ω_c	942	rad/s
ω_i	94	rad/s
ω_d	530	rad/s
ω_t	1.68e+03	rad/s
$\omega_{r\alpha}$	160	rad/s
ω_f	9.42e+03	rad/s
ω_r	172	rad/s
γ	0.5	-
Range	5000	μ m
$f_{sampling}$	10	KHz
$T_{simulink}$	$1/(10f_{sampling})$	s

A. Distortion

A good understanding of the error associated with quantization, known as distortion, can be gained from [18]. In this paper rounding quantization will be followed due to it's abundance in industry. A digital quantization level is defined as $Q = \frac{Range}{2^{bits}}$. Range is the maximum value that can be detected. Bits is related to the digitization of the data. This is the number of bits available to show the magnitude of the value. As an example, for a given sensor with a range of 1 nm several digitization processors are available, 5 bit and 6 bit. The 5 bit and 6 bit systems will result in a resolution of $\frac{1000nm}{2^5} = 31.25nm$ and $\frac{1000nm}{2^6} = 15.63nm$ respectively. The boundary between two Q's can be referred to as a jump or transition level. Observers can be implemented in order to estimate error. This can also be achieved by implementing reset control [23].

B. Performance deterioration

In order to show performance deterioration due to quantization a simulation is performed. The block diagram from Fig. 1 is followed. Let's consider a mass system with transfer function $\frac{1}{s^2}$ and controller settings from Table I. It was chosen to simulate a mass plant so the shape of the sensitivity function (S) would be predictable and deviations can be attributed to the controller instead of resonances or damping. A linear approach to S does not apply because there is a nonlinear element in the loop. Therefore the approach as defined in [28] is adopted, see Equation 7.

$$S_\sigma(\omega) = \frac{\max(|e(t)|)}{|R|} \quad \text{for } t \geq t_{ss} \quad (7)$$

Fig. 2 and Fig. 3 show some interesting behavior at low frequencies. Usually S tends to zero because the integrator has infinite gain at $\omega = 0$. Fig. 2 shows the steady state period for an input of 10 rad/s in the top. It can be seen that when quantization is introduced a sawtooth-like profile is present,

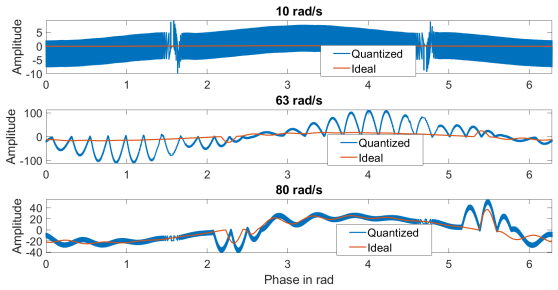

Fig. 2: The steady state period, with 9 bits quantization.

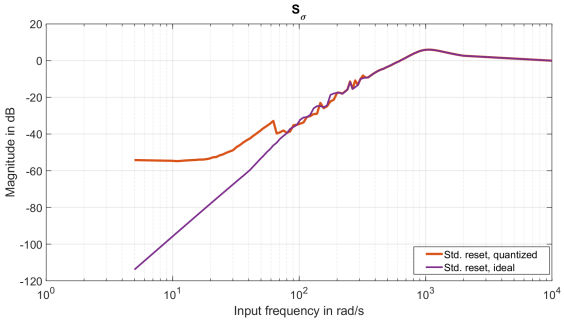

Fig. 3: S_σ for a mass system with 9 bits.

so $|S|$ will not go to zero for frequencies that approach zero. $|S|$ will level out to $|\frac{E}{Q}|$.

$S_{\sigma\ \text{quantized}}$ in Fig. 3 shows some additional behavior deterioration. An increased magnitude with respect to $S_{\sigma\ \text{ideal}}$ is seen in the form of a bump around 63 rad/s. The middle plot in Fig. 2 shows the response in the temporal domain. It can be seen that the increased magnitude is because of quantization induced excessive resetting. The resetting action is required around the bandwidth in order to achieve the phase advantage. For lower frequencies it is not essential.

See Equation 1, for quantization to cause a reset the mean of error has to be within $\frac{1}{2}Q \geq e \geq -\frac{1}{2}Q$. Within this error band quantization will cause zero-error crossings which are not present in the actual plant output y and thus could lead to performance degradation. If there were no quantization there would not be a distortion in the error and thus no excessive resets would occur.

IV. Reset Band as Solution for Quantization Induced Performance Deterioration

The reset band condition is a special case for a reset surface. Reset only occurs when the error enters the reset band. Fig. 4 shows an example where a reset band is applied to a CI. The standard CI resets when its input, the error, crosses zero. The CI with the reset band is seen to reset when the error enters the area of $|\delta|$ around zero.

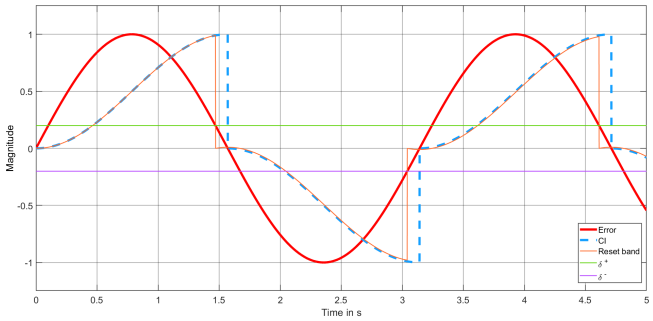

Fig. 4: The response of a Clegg integrator with and without reset band.

A. Reset band preliminaries

1) Definition: The reset band controller is defined as Equation 8 in [26].

$$R_\delta \begin{cases} \dot{\mathbf{x}}_r(t) = A_r\mathbf{x}_r(t) + B_r e(t) & \text{if } (e(t), \dot{e}(t)) \notin B_\delta \\ \mathbf{x}_r(t^+) = A_\rho \mathbf{x}_r(t) & \text{if } (e(t), \dot{e}(t)) \in B_\delta \\ u(t) = C_r\mathbf{x}_r(t) + D_r e(t) \end{cases} \quad (8)$$

where

$$\mathrm{B}_\delta = \{(x, y) \in \mathrm{R}^2 | (\mathrm{x} = -\delta \wedge \mathrm{y} > 0) \vee (\mathrm{x} = \delta \wedge \mathrm{y} < 0).$$

Reset band elements will be denoted with the subscript δ. So a reset band FORE will be FORE$_\delta$ where FORE$_0$ represent standard reset condition (with no reset band) as in FORE.

2) Sinusoidal Input Describing Function (SIDF): The reset band system can also be linearised with a SIDF. There is one major difference, for a reset band system the SIDF is a function of both input frequency and amplitude where the error $e = E\sin(\omega t)$. This is because the amplitude of the sinusoidal input also determines when the reset occurs. The zero-error crossings are still at the same phase, but crossings of non-zero values are influenced by amplitude. If δ is defined as $\delta = c\ E$ instead of $\delta = c$ the amplitude dependence is removed with regard to the reference, the dependence for noise and disturbance remains. The SIDF for a full reset FORE$_\delta$ with input $e = E\sin(\omega t)$ is given in [26]. However, in order generalize the DF such that partial reset is included the method of [28] has been applied. Instead of a phase shift of the error because of a LPF the reset band causes a phase shift because it resets at a prescribed amplitude. Equation 9 gives the DF as stated in [28]. In the application of a reset band only ϕ has been redefined in this paper.

$$C_r\left(j\omega I - A_r\right)^{-1}\left(I + e^{j\phi} j\Theta_s(\omega)\right)B_r + D_r \quad (9)$$

Where

$$\Theta_s = \Theta_\rho\left(\frac{-A_r\sin\phi + \omega\cos\phi I}{\omega}\right)$$

and

$$\phi = \pi - \sin^{-1}\left(\frac{\delta}{E}\right).$$

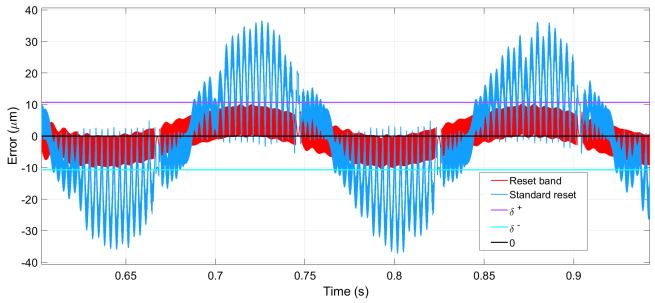

Fig. 5: Steady state response of a mass system with and without reset band.

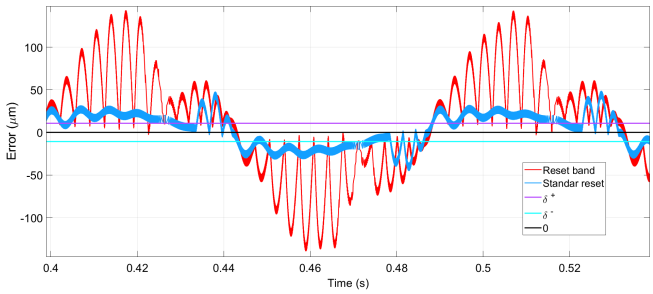

Fig. 6: Steady state response of a mass system with and without reset band.

3) Stability: A stability analysis of reset control systems with a reset band is conducted in [29]. An important note is that when $\frac{\delta}{E}$ tends towards 1 limit cycling might occur.

B. Reset band applied in simulation

In order to show that the reset band can be a valid solution the mass system and controller from the earlier simulations are taken once again. A sinusoid reference with an amplitude of 5000μm and frequency of 40 rad/s was applied with a numerical range of 5000μm and 9 bits, leading to Q $= \frac{5000}{2^9}$. For a steady state δ is designed such that it is bigger than the maximum error in addition to Q. This leads to a required reset band of $\delta \approx 10.7\mu$m, which was applied.

The time response in red in Fig. 6 shows that the reset band solution can cause performance deterioration if improperly tuned. The reference was a sine with amplitude of 5000μm and frequency of 70 rad/s. For a standard reset condition the contribution of quantization to the error is relatively low, so quantization does not induce resets for a large part of the reference period. Let's now consider the case of the reset band. For the reset band controller δ was specifically tuned for a lower frequency such that the error lies fully within the band. Following the theoretical understanding of the sensitivity function, a higher frequency should in this case induce a larger error. This increased error is able to cross the reset band and therefore resets will be induced. These resets can be undesired and cause performance degradation. In this situation the ratio of $\frac{E}{\delta}$ will tend towards 1. According to [29] this can cause limit cycling. Therefore proper tuning is essential and tuning guidelines have been given in the next section.

C. Tuning guidelines

In section III-B performance degradation was identified. Problems occurred at lower frequencies when quantization induced resets. This leads to the desire to have a linear controller for lower frequencies and a reset controller around bandwith to get the phase advantage.

From theory the maximum quantization can be derived [18]. This is stated in Lemma 1.

***Lemma** 1:*

- Rounding quantization can cause a maximum error of $\pm\frac{1}{2}Q$ relative to the true error.
- Truncation quantization can cause a maximum error of $+Q$ relative to the true error.

With Lemma 1 a linear domain in the frequency domain can be designed based on a reference amplitude, see Lemma 2.

***Lemma** 2:* There will be no reset for $\omega < \omega_s$ if the following condition is satisfied:

$$\delta = \max(e)\,|_{\omega_s} + \frac{Q}{2} \tag{10}$$

Where: $\max(e)\,|_{\omega<\omega_s} = |S|_{\text{BLS}} \cdot |r|$, since $|S|_{=}|\frac{e}{r}|$.

***Assumption** 1:* For Lemma 2 the assumption was made that there is no anti-resonance below bandwith and therefore S is smoothly increasing. In this theoretical approach there is assumed to be no noise or disturbance present. Also, no observer is applied.

***Remark** 1:* Since a controller only responds to the distorted signal y, which is identical for both quantization types, Lemma 2 holds both for truncation and rounding quantization.

1) Noise and disturbances: Noise will be present in practice. If δ is tuned too tightly noise can induce error crossings of δ. To resolve this a safety factor can be implemented, or a noise identification can be used to find the maximum noise amplitude which can be added to δ. Disturbances can be a problem as well. Disturbances would be measured in the identification, but it can also be deduced if a disturbance model is available.

The process sensitivity function $\frac{e}{d} = GS$ can be used in order to estimate the error as a result of the disturbance. Plant uncertainties along with the fact that the DF is used to predict the error means that a safety margin should be applied to δ:

$$\delta_{robust} = k\delta.$$

Where k is a safety factor of $k \geq 1$. From here on δ is the applied reset band magnitude with an applied safety margin.

TABLE II: Controller settings applied to the mass stage

P	6.0954e+05	-
ω_c	942	rad/s
ω_i	94	rad/s
ω_d	530	rad/s
ω_t	1.68e+03	rad/s
$\omega_{r\alpha}$	160	rad/s
ω_f	9.42e+03	rad/s
ω_r	172	rad/s
γ	0.5	-
Range	5000	μ m
$f_{sampling}$	10	KHz
$T_{simulink}$	$10/f_{sampling}$	s

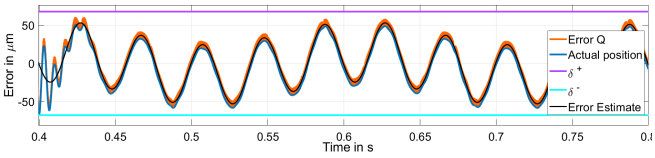

Fig. 7: Controller output and error for a double sine reference.

2) Multiple Sinusoid Reference / Sinusoidal Decomposition of Reference: In practice there are many situations where a reference exists out of multiple sines, e.g. a 4th order trajectory [30]. Therefore it is imperative that this solution holds for superposition. Because a reset system is nonlinear superposition does not always hold. However, with the designed tunable linearity range the following remark can be made:

***Remark** 2:* Within the reset band the system is linear so as long as the error is within the reset band superposition holds.

Figure 7 shows the steady state response for the controller of Table II applied to the mass system. It can be seen in Fig. 7 that the actual position, shown in blue, has $-\frac{1}{2}Q$ offset w.r.t. the estimated error, shown in black. This is due to truncation quantization. The reference was a summation of two sines with $A_1 = 5000\mu$m, $A_2 = \frac{1}{3} \cdot 5000\mu$m, $f_1 = 5$ Hz and $f_2 = 25$ Hz. The sensitivity function was used to estimate the error for each individual sine which were summed.

A Fourier decomposition can be used to convert references to sines. Normally, the magnitudes of the higher orders of a Fourier decomposition are diminishing quickly. For the application discussed here the higher orders of the Fourier decomposition can still be imperative. When regarding a sensitivity function, e.g. Fig. 8, a rising slope can be seen. This rising slope amplifies the relative magnitudes of the higher orders.

D. Numerical sensitivity function

To analyze the sensitivity function the same mass system as before is taken. Fig. 8 shows the performance of the solution. It can be seen that an improvement is achieved at lower frequencies. Moreover, the end of the linear frequency range from Lemma 2 can be found at $\omega_s \approx 50$ rad/s. A variable or adaptive reset band as discussed in [26] could overcome this

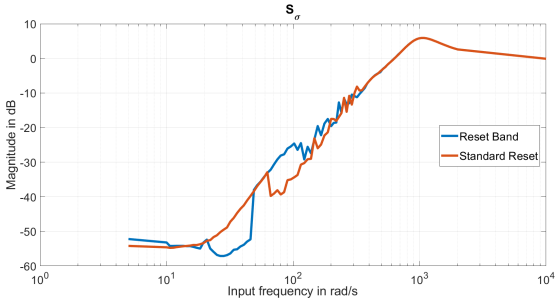

Fig. 8: S_σ with quantization for reset band and standard reset.

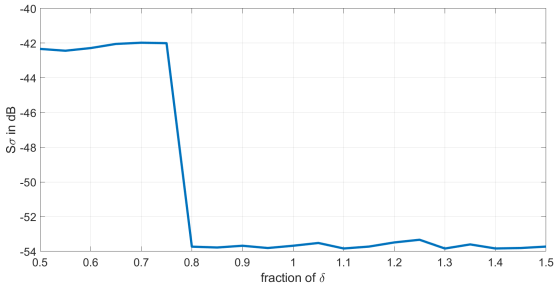

Fig. 9: S_σ vs delta for a quantized reference.

issue. Another method would be to apply a LPF such that δ quickly diminishes after a predetermined frequency.

E. Sensitivity to δ

To analyze the sensitivity of the tuning method a series of numerical experiments was performed. A sinusoid reference of with $A = 5000\mu$m and f ≈ 6.4Hz was applied to the mass system of before. δ was calculated according to Equation 10 to be $16\mu\text{m} \approx 5000\mu\text{m} \cdot -58.6dB + \frac{1}{2} \cdot \frac{5000\mu\text{m}}{2^9}$. The results are plotted in Fig. 9 where it can be seen that there is a hard border where δ is suddenly no longer beneficial, this is the case when the error starts to touch the reset band in steady state. This hard edge is also visible in Fig. 8. This is the case when the peak of the sinusoidal output of the quantized signal touches the reset band. This shows that the solution of reset band is not robust if the reference frequency is close to ω_s.

V. Practical Validation

A. Precision positioning stage

The system used for validation is a custom designed one-degree-of-freedom high precision positioning stage, see Fig. 10. Essentially it is a mass-spring system. It has a Lorentz actuator and a Renishaw RLE10 laser encoder set to 10 nm resolution. An FPGA NI cRIO system was implemented to achieve fast real-time control with a sampling rate of 10 kHz.

As is common in industry, frequency response data of the system is obtained by applying chirp signals. The results can be seen in Fig. 11. The following transfer function was found:

$$\frac{3.038e04}{s^2 + 0.7413s + 243.3}.$$

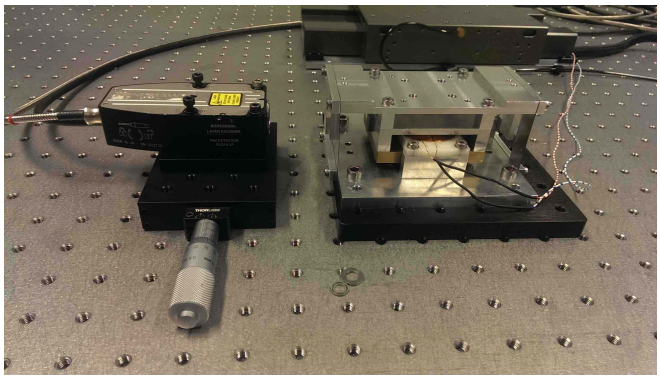

Fig. 10: Fine positioning stage.

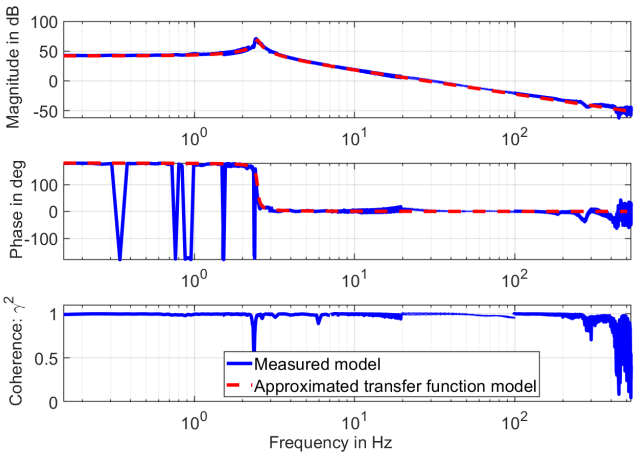

Fig. 11: Frequency response data and estimated model.

B. Designed controller

It was decided to study CgLp-PID controller for a bandwidth (defined as crossover frequency) of 150 Hz and phase margin of 40°. The CgLp-PID was designed according to the transfer function of Equation 6 with the parameters shown in Table III. The controller was discretized according to the tustin method.

C. Results

To show that the quantization induced performance degradation does not occur for one specific Q, two Q's have been implemented. The higher resolution is when 1 increment (inc)

TABLE III: Controller settings for practical application.

P	16.41	-
γ	0	-
ω_c	942.5	rad/s
ω_i	94.25	rad/s
ω_d	529.2	rad/s
ω_t	1679	rad/s
$\omega_{r\alpha}$	697.6	rad/s
ω_r	812.1	rad/s
ω_f	9420	rad/s

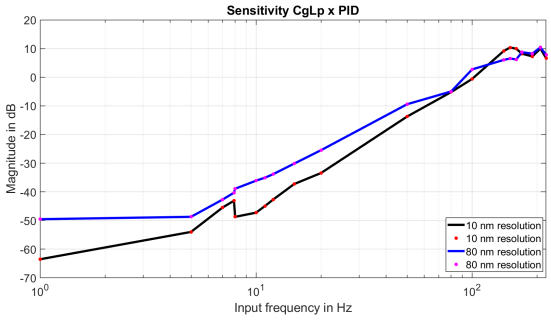

Fig. 12: Experimentally deduced sensitivity functions for CgLp-PID with 10 nm and 80 nm resolutions.

corresponds to 10 nm. A second resolution was chosen to correspond to 80 nm.

1) 1 increment resolution: For the low frequencies a reference amplitude of 30μm was applied. This leads to a theoretical limit of -69 dB for a steady state 1 inc. (10 nm) error. In practice there were some noise and disturbances, therefore the theoretical limit was at 2 inc. error with -63 dB.

For the full resolution setup the quantization induced problems occurred at the low frequency range. When regarding Fig 12 a bump similar to Fig. 8 can be seen to start from 5 Hz and drop at 8 Hz where the problematic region was left.

It was not possible to do a representative sensitivity plot for the reset band. Due to the small stroke of the stage in combination with saturation the 30μm reference amplitude was not achievable for all frequencies. For the standard reset system the reference amplitude could be decreased at higher frequencies because the amplitude dependence of the response is minimal. However, the reset band system has a more pressing amplitude dependence that is inherent of the reset condition.

In Fig. 13 the steady state time response at 7.9 Hz is shown in blye. It can be seen that at first the error is 200 nm (-43.5 dB) due to excessive resetting. When at 2.75 s a reset band of $\delta = 8$ inc. is initiated the error reduces to 70 nm (-52.6 dB). Therefore for this frequency the reset band solution against quantization induced performance degradation leads to an improvement of 9 dB. As can be seen in red in Fig. 13 the response when purposefully mistuning δ in shows performance degradation. The response is only plotted from when the reset band was initiated. In this case no benefits from the reset band are found. However neither are the drawbacks as detrimental as seen in some simulations.

2) 8 increment resolution: Once again a reference amplitude of 30μm was applied for lower frequencies. The theoretical limit is then -51.5 dB. In this case the theoretical and practical limit nicely agree because the noise level is small relative to the 80 nm resolution. In Fig. 12 the deduced sensitivity function for a standard reset condition is shown. In this case no bump can be seen, however quantization still induced performance degradation. As is shown in Fig. 14. Implementing a reset band with $\delta = 15$ inc. results in an improvement of 6 dB. As can be seen in Fig. 14 for this resolution a badly tuned reset band will cause performance

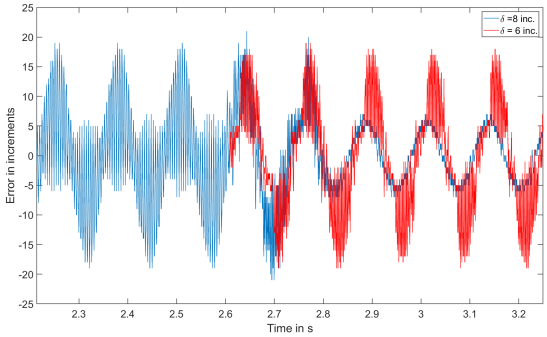

Fig. 13: Steady state time response at 7.9 Hz, 1 inc. resolution which corresponds to 10nm. At t=2.6s reset band is initiated.

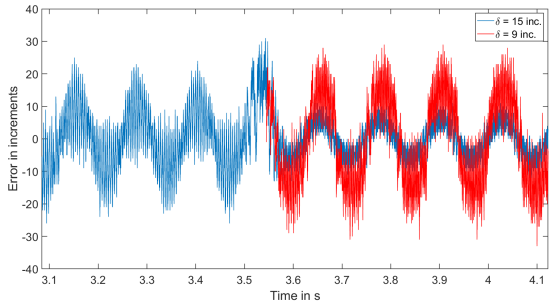

Fig. 14: Steady state time response at 7.9 Hz, 8 inc. resolution which corresponds to 80nm. At t=3.5s reset band is initiated.

degradation. A degradation of 2 dB was recorded. Once again the response of the second δ was only plotted after initiation.

VI. Conclusion

Reset control has been around for quite some time and has been implemented in various applications. However, there has been no focus on quantization. In this paper it is shown that quantization can degrade performance for reset controllers.

Reset band is proposed as a solution for quantization induced performance degradation. Tuning guidelines are provided. Experiments have validated that a reset band can greatly reduce quantization induced performance degradation. In one case the error was reduced from 200 nm to less than 80 nm. However, when improperly tuned the reset band can cause further performance degradation. Moreover, a reset band can either improve or degrade noise attenuation performance.

An interesting direction of research would be to investigate whether real time adapted δ, e.g. in the form of a variable or advanced reset band, could improve quantization performance degradation farther. Also, the implementation of an observer can reduce distortion and thus result in a smaller value for δ.

Acknowledgment

The authors would like to thank Hittech Multin. This work was supported by NWO, through OTP TTW project #16335.

References

[1] H. W. Bode, *Network Analysis and Feedback Amplifier Design*. Princeton: van Nostrand New York.

[2] J. C. Clegg, "A nonlinear integrator for servomechanisms," *Transactions of the American Institute of Electrical Engineers, Part II: Applications and Industry*, vol. 77, no. 1, pp. 41–42, 2013.

[3] I. Horowitz and P. Rosenbaum, "Non-linear design for cost of feedback reduction in systems with large parameter uncertainty," *International Journal of Control*, vol. 21, no. 6, pp. 977–1001, 1975.

[4] L. Hazeleger, M. Heertjes, and H. Nijmeijer, "Second-order reset elements for stage control design," *Proceedings of the American Control Conference*, vol. 2016-July, pp. 2643–2648, 2016.

[5] S. H. HosseinNia, I. Tejado, and B. M. Vinagre, "Fractional-order reset control: Application to a servomotor," *Mechatronics*, vol. 23, no. 7, pp. 781–788, oct 2013. [Online]. Available: https://linkinghub.elsevier.com/retrieve/pii/S0957415813000470

[6] A. Ba and A. Vidal, "Definition and tuning of a PI + CI reset controller," pp. 4792–4798, 2007.

[7] Y. Guo, Y. Wang, and L. Xie, "Frequency-domain properties of reset systems with application in hard-disk-drive systems," *IEEE Transactions on Control Systems Technology*, vol. 17, no. 6, pp. 1446–1453, 2009.

[8] N. Saikumar, R. K. Sinha, and S. H. HosseinNia, ""Constant in Gain Lead in Phase" Element– Application in Precision Motion Control," *IEEE/ASME Transactions on Mechatronics*, vol. 24, no. 3, pp. 1176–1185, jun 2019. [Online]. Available: https://ieeexplore.ieee.org/document/8681086/

[9] A. Vidal and A. Baños, "Reset compensation for temperature control: Experimental application on heat exchangers," *Chemical Engineering Journal*, vol. 159, no. 1-3, pp. 170–181, 2010.

[10] H. Li, C. Du, and Y. Wang, "Optimal reset control for a dual-stage actuator system in HDDs," *IEEE/ASME Transactions on Mechatronics*, vol. 16, no. 3, pp. 480–488, 2011.

[11] H. Li, C. Du, Y. Wang, and Y. Guo, "Discrete-time optimal reset control for hard disk drive servo systems," *IEEE Transactions on Magnetics*, vol. 45, no. 11, pp. 5104–5107, 2009.

[12] Y. Zheng, Y. Chait, C. Hollot, M. Steinbuch, and M. Norg, "Experimental demonstration of reset control design," *Control Engineering Practice*, vol. 8, no. 2, pp. 113–120, feb 2000. [Online]. Available: https://linkinghub.elsevier.com/retrieve/pii/S0967066199001318

[13] F. S. Panni, H. Waschl, D. Alberer, and L. Zaccarian, "Position regulation of an EGR valve using reset control with adaptive feedforward," *IEEE Transactions on Control Systems Technology*, vol. 22, no. 6, pp. 2424–2431, 2014.

[14] A. Palanikumar, N. Saikumar, and S. H. Hosseinnia, "No More Differentiator in PID: Development of Nonlinear Lead for Precision Mechatronics," in *2018 European Control Conference, ECC 2018*. IEEE, jun 2018, pp. 991–996. [Online]. Available: https://ieeexplore.ieee.org/document/8550088/

[15] ——, "No More Differentiator in PID : Development of Nonlinear Lead for Precision Mechatronics."

[16] L. Chen, N. Saikumar, S. Baldi, and S. H. Hosseinnia, "Beyond the Waterbed Effect : Development of Fractional Order CRONE Control with Non-Linear Reset," 2019.

[17] "Quantization," in *Digital Video and HD*. Elsevier, 2012, pp. 37–46. [Online]. Available: https://linkinghub.elsevier.com/retrieve/pii/B9780123919267500047

[18] D. Rauth and V. Randal, "Analog-to-digital conversion. part 5," *IEEE Instrumentation & Measurement Magazine*, vol. 8, no. 4, pp. 44–54, oct 2005. [Online]. Available: http://ieeexplore.ieee.org/document/1634987/ http://ieeexplore.ieee.org/document/1518622/

[19] E. Lai, "Converting analog to digital signals and vice versa," *Practical Digital Signal Processing*, pp. 14–49, 2003.

[20] F. Ferrante, "On quantization and sporadic measurements in control systems: stability, stabilization, and observer design," *Dissertation*, 2015.

[21] F. Minyue, "Quantization for feedback control and estimation," *Proceedings of the 27th Chinese Control Conference, CCC*, pp. 751–756, 2008.

[22] J. H. Park, H. Shen, X. H. Chang, and T. H. Lee, "Quantized static output feedback control for discrete-time systems," *Studies in Systems, Decision and Control*, vol. 170, no. 8, pp. 41–67, 2019.

[23] J. Zheng and M. Fu, "A reset state estimator using an accelerometer for enhanced motion control with sensor quantization," *IEEE Transactions on Control Systems Technology*, vol. 18, no. 1, pp. 79–90, 2010.

[24] H. Zhu and H. Fujimoto, "Overcoming current quantization effects for precise current control using dithering techniques," *IEEJ Journal of Industry Applications*, vol. 2, no. 1, pp. 14–21, 2013.

[25] A. Barreiro, A. Banos, and S. Dormido, "Reset Control Systems with Reset Band: Well-posedness and Limit Cycles Analysis," in *2011 19th Mediterranean Conference on Control & Automation (MED)*. IEEE, jun 2011, pp. 1343–1348. [Online]. Available: http://ieeexplore.ieee.org/document/5983109/

[26] A. Baños and A. Barreiro, *Reset Control Systems*, ser. Advances in Industrial Control. London: Springer London, 2012. [Online]. Available: http://link.springer.com/10.1007/978-1-4471-2250-0

[27] C. Prieur, I. Queinnec, S. Tarbouriech, and L. Zaccarian, "Analysis and synthesis of reset control systems," Ph.D. dissertation, 2018.

[28] C. Cai, A. A. Dastjerdi, N. Saikumar, and S. H. Hosseinnia, "The optimal sequence for reset controllers."

[29] A. Baños, S. Dormido, and A. Barreiro, "Stability analysis of reset control systems with reset band," *IFAC Proceedings Volumes (IFAC-PapersOnline)*, vol. 3, no. PART 1, pp. 180–185, 2009.

[30] P. Lambrechts, M. Boerlage, and M. Steinbuch, "Trajectory planning and feedforward design for electromechanical motion systems," *Control Engineering Practice*, vol. 13, pp. 145–157, 2005.

4

Time Regularization

This chapter is in in paper format. The paper proposes time regularization as a solution for quantization induced performance degradation. The paper is planned to be submitted to the 2021 European Control Conference (ecc21).

4.1. Time regularization paper

Time regularization as a solution to mitigate quantization induced performance degradation

Bas Kieft, Niranjan Saikumar, and S. Hassan HosseinNia *Senior Member, IEEE*

***Abstract*—Reset control is known to be able to outperform PID. However, for motion control systems quantization can cause severe performance degradation. This paper shows the application of time regularization for a novel purpose. Tuning guidelines for the time regularization parameter are provided.**

Numerical simulations have been conducted in matlab simulink on a mass system in order to analyze the cause of the quantization induced performance degradation. Moreover a performance and robustness analysis was performed. Experiments have been conducted on a high level motion system for validation.

It is estimated by numerical simulations that time regularization can reduce quantization induced performance degradation by almost 10 dB. Experiments have shown a reduction of several dB for a high tech motion stage.

Our study reveals that the application of time regularization can significantly reduce quantization induced performance degradation.

***Index Terms*—Reset Control, Time Regularization, Mechatronics, Motion Control, Implementation, Quantization.**

I. Introduction

OVER the past years reset control has increased in popularity as a complement to linear Proportional-Integral-Differential (PID) control. This is because the reset action allows the controller to surpass the limitations as posed by Bode [1]. Beker et al. were the first to demonstrate that reset control is able to outperform linear control [2].

Reset control was introduced by Clegg in the form of a Clegg Integrator (CI) [3]. CI is an integrator that resets the state to zero when the input is zero. Thus the phase lag is reduced from -90° to -38°. The First Order Reset Element (FORE) was created as a continuation in reset control [4]. The FORE is a nonlinear low-pass filter (LPF), the Second Order Reset Element (SORE) is a second order FORE [5]. Fractional control was integrated with a CI in [6]. This further increased the tunability of reset control elements.

Some of the earlier elements introduced variables in order to tune the influence of nonlinearity by frequency, such that the element's output remained linear for a part of the frequency domain [4], [5]. Other methods to tune nonlinearity is by the application of hybrid control and partial reset. These methods alter the after reset value. A CI in tandem with an I result in a PI+CI element [7]. In a full reset controller the state of the integrator is reset to 0. Partial reset allows the state of the integrator to be reset to a predetermined fraction. This is can be introduced to a FORE element, which creates a Generalized FORE (GFORE) [8] or to a SORE creating a Generalized SORE (GSORE) [9]. Fractional control in reset control was advanced in [10] with the introduction of the Generalized Fractional Order Reset Element (GFrORE).

The benefits of reset control are significant. It has been applied in process industry and motion control. A PI+CI element was applied to an industrial heat exchanger in [11]. Furthermore, this paper researches the application of a variety of reset conditions. A precision instrument where positioning speed is crucial for performance is a Hard Disk Drive (HDD). In [12], [13] and [8] HDD are used as a universal base for reset control research. Many motor control applications use servo motors, [6] has done research into the application of reset control in this field. Moreover, applications of reset control span the field from tape-speed setups [14] to exhaust gas re-circulation [15].

The CI allows the reset elements to decrease the phase lag that is introduced by an integrator. However, more interesting elements can be created by carefully combining existing elements. the Constant in gain Lead in phase (CgLp) [9], [16] element is an excellent example. this element combines a GFORE with a linear lead element to achieve an increase in phase while not altering the gain. A second order CgLp is possible by implementing a GSORE element.

The frequency domain approach is the most widely used method in industry. However, this is a linear approach so reset elements have to be linearized in order to use this method. Sinusoidal Input Describing Function (SIDF) is a common linearization that is introduced with the CI. This approach was adopted for all discussed elements [3], [4], [5], [6], [7], [8], [9], [16].

In most cases in literature, results are extracted from simulations where normally continuous time implementations are used. In [17], [18], [9] the controllers were discretized. Normally the steps associated with practical implementation do not cause issues. However, quantization is a type of practical issue that is not studied.

Quantization is a form of signal distortion that is often compared to, or included in noise. It has been researched extensively, e.g. [19], [20], [21]. Its influence on linear control is well known [22], [23], [24]. Reset control has been shown to have superior noise attenuation properties due to the possibility of decreasing high frequency gain [17], [18], [9]. However, the effects that quantization can have on reset

control is not well studied. Some research in quantization combined with reset control was done in [25] where the state estimator had reset elements in order to mitigate quantization generated signal distortion. Generally quantization is modeled as white or colored noise [26]. However, this does not represent reality. For example, the frequency of distortion is dependent on the quantizer resolution and response slope.

Convergence has been proved for the traditional zero error crossing reset condition as stated by [3]. Moreover, the DF method can be applied. However, other reset conditions do exist. An interesting technique to tune the range of nonlinearity is a temporal approach. Time regularization was introduced as a method to overcome Zenoness [27]. Zenoness is when a theoretical system gets stuck in time and cannot advance. Time regularization was not invented for reset control specifically. In [28] time regularization is used in order to avoid Zenoness in reset control. This approach is essentially a method where a holding function is applied to the reset condition such that resets are not induced within this holding period. In practical setups Zenoness will not occur due to among other discretization. However, this same concept can be used to overcome the performance deterioration that occurs due to quantization.

The main contributions of this paper are a proposed solution for quantization induced problems based on the application of time regularization and a method to tune the proposed solution.

The paper is structured as follows: Section II states the preliminaries required for the paper. Then in section III the performance degradation is expanded upon. Section IV proposes a solution for the performance degradation with tuning rules proposed in section IV-B. A conclusion is provided in section VI.

II. Preliminaries

A. Reset Control Definition

For this research paper the definition stated in [29] will be followed. This definition has been expanded upon such that it leads to the form seen in Equation 1, e.g. [9] and [8].

$$(R): \quad \begin{cases} \dot{\mathbf{x}}_r(t) = A_r\mathbf{x}_r(t) + B_r e(t) & \text{if } e(t) \neq 0 \\ \mathbf{x}_r(t^+) = A_\rho \mathbf{x}_r(t) & \text{if } e(t) = 0 \\ u(t) = C_r\mathbf{x}_r(t) + D_r e(t) \end{cases} \tag{1}$$

where $\mathbf{x}_r(t)$ are the reset states, u is the output of the reset controller and A_r, B_r, C_r and D_r are the state space matrices and are referred to as the base linear system. A_ρ is diagonal and is the reset matrix that determines the states to be reset and their after reset value. For a full reset A_ρ is the zero matrix and for a linear controller, this is the identity matrix.

B. Describing Function

Because reset control is nonlinear a Sinusoidal Input Describing Function (SIDF) analysis can be applied such that the reset control element is approximated. The adaption of [8] performed in [9] presents the describing function for the reset element of Equation 1 as:

$$G(j\omega) = C_r^T(j\omega I - A_r)^{-1}(I + j\Theta_\rho(\omega))B_r + D_r \tag{2}$$

where

$$\Theta_\rho \triangleq \frac{2}{\pi}\left(I + e^{\frac{\pi A_r}{\omega}}\right)\left(\frac{I - A_\rho}{I + A_\rho e^{\frac{\pi A_r}{\omega}}}\right)\left(\left(\frac{A_r}{\omega}\right)^2 + I\right)^{-1} \tag{3}$$

C. Stability

The stability of reset control has been investigated and necessary conditions can be found in [29]. The method detailed here is known as the H_β condition.

Of the closed loop system with dimension $n = n_p + n_r$ where n_r signifies the number of states being reset and the subscript p for the elements denote that these are for the plant the state can be described as:

$$\mathbf{x} = \begin{bmatrix} \mathbf{x}_p \\ \mathbf{x}_r \end{bmatrix},$$

The closed loop system is then:

$$\begin{cases} \dot{\mathbf{x}}(t) = A_{cl}\mathbf{x}(t) & \text{if } e(t) \neq 0 \\ \mathbf{x}(t^+) = A_R\mathbf{x}(t) & \text{if } e(t) = 0 \end{cases}$$

where

$$A_{cl} = \begin{bmatrix} A_p & B_pC_r \\ -B_rC_p & A_r \end{bmatrix}$$

and

$$A_R = diag(I_{np}, A_\rho)$$

A_{cl} denotes the closed loop A-matrix.

For a reset controller defined as Equation 1 the system is quadratically stable if there exists a constant $\beta \in \mathbb{R}^{n_p \times 1}$ and a positive definite $P_\rho \in \mathbb{R}^{n_r \times n_r}$ such that the restricted Lyapunov Equation (4, 5) has a solution for P.

$$P > 0, \quad A_{cl}^T P + P A_{cl} < 0 \tag{4}$$

$$B_0^T P = C_0 \tag{5}$$

where

$$C_0 = \begin{bmatrix} \beta C_p & 0_{n_r \times n_{nr}} & P_\rho \end{bmatrix}, B_0 = \begin{bmatrix} 0_{n_p \times n_{nr}} \\ 0_{n_{nr} \times n_r} \\ I_{nr} \end{bmatrix}$$

and n_{nr} stands for the number of non-resetting states.

D. Reset Elements

1) Clegg integrator: The CI was invented in 1958 [3]. Following the definition of Equation 1 the CI is defined as $A_r = 0$, $B_r = 1$, $C_r = 1$, $D_r = 0$ and $A_\rho = 0$.

2) FORE: To offer a tunable frequency range of nonlinearity the First Order Reset Element (FORE) was invented [4]. The FORE is essentially a non-linear low-pass filter (LPF) with corner frequency ω_r. Following the definition of Equation 1 the FORE is defined as $A_r = -\omega_r$, $B_r = \omega_r$, $C_r = 1$, $D_r = 0$ and $A_\rho = 0$. A generalisation for FORE (GFORE) has been defined in [8] where $A_\rho = \gamma$ with $-1 \leq \gamma \leq 1$ makes GFORE a partial reset element. $\gamma = 1$ represents a base linear low-pass filter.

3) SORE: The Second Order Reset Element (SORE) was introduced in [5]. SORE has been defined according to Equation 1 with the following matrices:

$$A_r = \begin{bmatrix} 0 & 1 \\ -\omega_r^2 & -2\beta_r\omega_r \end{bmatrix}, B_r = \begin{bmatrix} 0 \\ \omega_r^2 \end{bmatrix},$$
$$C_r = \begin{bmatrix} 1 & 0 \end{bmatrix}, D_r = \begin{bmatrix} 0 \end{bmatrix}.$$

where β_r is the damping coefficient. SORE has been adjusted to allow for partial reset in the GSORE element [9].

4) Constant in gain Lead in phase element: An element with high potential is the Constant in gain Lead in phase element (CgLp). This element has a linear and nonlinear range. In the nonlinear range CgLp adds phase without altering the gain [9], [16]. CgLp is essentially a FORE element in combination with a linear lead. Using SORE a second order CgLp can be realized. The state space representation of CgLp is:

$$A_r = \begin{bmatrix} -\omega_{r\alpha} & 0 \\ \omega_f & -\omega_f \end{bmatrix}, B_r = \begin{bmatrix} \omega_{r\alpha} \\ 0 \end{bmatrix},$$
$$C_r = \begin{bmatrix} \frac{\omega_f}{\omega_r} & (1 - \frac{\omega_f}{\omega_r}) \end{bmatrix}, D_r = \begin{bmatrix} 0 \end{bmatrix},$$
$$A_\rho = \begin{bmatrix} \gamma & 0 \\ 0 & 1 \end{bmatrix}.$$

where $\omega_{r\alpha}$, ω_f and ω_r are the corner frequencies for the FORE, linear LPF and linear lead respectively. γ indicates a possible partial reset.

E. CgLp-PID

The CgLp element is best used in combination with a PID controller. CgLp-PID is a CgLp element multiplied with a linear PID controller, in this paper the choice was made to follow the CgLp · PID order. The design procedure is stated in [9]. It is required to have a stable base linear system.

CgLp, having the constant gain but lead in phase, can be used to partially or completely replace the D part of PID. A CgLp-PID can be represented as:

$$\underbrace{P(1+\frac{\omega_i}{s})}_{PI}\underbrace{\frac{(s/\omega_d+1)}{(s/\omega_t+1)}}_{D}\underbrace{\frac{1}{s/\omega_{r\alpha}+1}^{\gamma}\frac{s/\omega_r+1}{s/\omega_f+1}}_{CgLp} \quad (6)$$

The phase lead provided by D can be tuned by varying a in $\omega_d = \omega_c/a$ and $\omega_t = \omega_c a$. The phase lead provided by CgLp can be tuned by ω_r and γ. With sufficiently small ω_r and $\gamma = 0$ it is possible to provide 52° phase lead.

TABLE I: Controller settings applied to the mass stage.

P	6.0954e+05	-
ω_c	942	rad/s
ω_i	94	rad/s
ω_d	530	rad/s
ω_t	1.68e+03	rad/s
$\omega_{r\alpha}$	160	rad/s
ω_f	9.42e+03	rad/s
ω_r	172	rad/s
γ	0.5	-
Range	5000	μ m
$f_{sampling}$	10	KHz
$T_{simulink}$	$1/(10f_{sampling})$	s

III. Quantization induced performance deterioration

1) Block diagram: the block diagram of control to be studied in this paper is shown in Fig. 1.

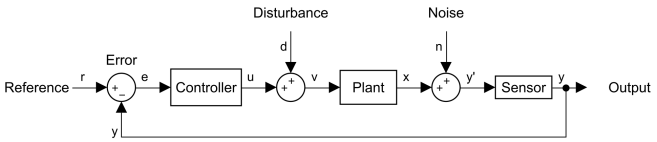

Fig. 1: Block diagram definition.

A. Distortion

The error associated with quantization is known as distortion. A good understanding can be gained from [20]. Due to it's abundance in industry rounding quantization will be followed in this paper. A quantization level is defined as $Q = \frac{Range}{2^{bits}}$. Range is described as the maximum value that can be detected. Bits is related to the digitization of the data and is the number of bits available to show the magnitude of the value. As an example, for a sensor with a range of $1000nm$ several digitization processors are available, 5 bit and 6 bit. The 5 bit and 6 bit systems will result in a resolution of $\frac{1000nm}{2^5} = 31.25nm$ and $\frac{1000nm}{2^6} = 15.63nm$ respectively. The boundary between two Q's can be referred to as a jump or transition level.

B. Performance deterioration

To show that distortion causes performance degradation a mass system with transfer function $\frac{1}{s^2}$ and controller settings from Table I is analyzed. A mass system has predictable behavior for the sensitivity function (S), so any aberration indicates deviated controller behavior. A normal sensitivity function analysis does not fully hold due to nonlinearities. To properly analyze S the gain has been calculated with a steady state period. This leads to S_σ in a method established in [30] that is shown in Equation 7.

$$S_\sigma(f) = \frac{\max(|e(t)|)}{|r|} \quad \text{for } t \geq t_{ss} \quad (7)$$

where $r = A\sin(f\ 2\pi t)$ and $e = E\sin(f\ 2\pi t + \phi)$ with ϕ being a shift in phase.

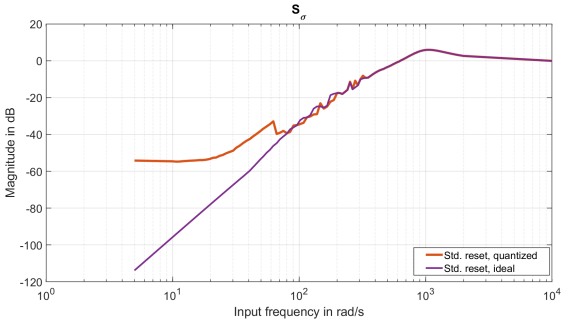

Fig. 2: S_σ for a mass system with 9 bits.

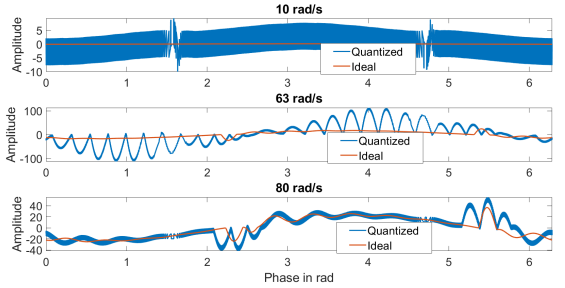

Fig. 3: The steady state period, with 9 bits.

In Fig. 2, S_σ for this system can be seen. For a properly tuned controller S would go to zero. Be that as it may, when quantization is at play the steady state error can never go below Q. This leads to an altered S that has a theoretical limit at $|\frac{E}{Q}|$. Fig. 3 shows the steady state period for an input of 10 rad/s. It can be seen that when quantization is introduced a sawtooth-like profile is present, so $|S|$ will not go to zero for frequencies that approach zero. $|S|$ will level out to $|\frac{E}{Q}|$.

As can also be seen in Fig. 3 especially the response for 63 rad/s shows a significant difference in response between quantized and ideal sensors. This is due to quantization induced excessive resetting. In Fig. 2 this shows as a break in the expected +2 slope trendline; a bump can be seen.

When reviewing Equation 1, it can be deduced that a quantization jump, which has a magnitude of $\frac{1}{2}Q$ with respect to the mean of the error, can only induce reset when the mean of the error is within $\frac{1}{2}Q \geq e \geq -\frac{1}{2}Q$.

IV. Time Regularization as Solution for Quantization Induced Performance Degradation

A. Time regularization preliminaries

Performance deterioration was established in section III-B. The problem was excessive resetting. In literature a similar phenomenon is discussed known as Zenoness [29]. A Zeno-solution is when an infinite number of discrete transitions take place in a finite amount of time. Although Zeno solution does not occur in practice due to discretization, the solution proposed in [27] is useful to solve the quantization problem. Quantization causes performance deterioration by initiating an excessive amount of resets in a tight sequence. A holding time will prevent subsequent resets and thus improve performance.

This paper brings novelty to the time regularization field by showing that it can mitigate quantization induced performance degradation. Moreover, tuning guidelines are provided with an explanation of the consequences of mistuning.

1) Definition: A generally adopted definition of time regularization can be found in Equation 8 from [29].

$$R_\rho : \begin{cases} \dot{\tau} = 1,\ \dot{\mathbf{x}}_r(t) = A_r\mathbf{x}_r(t) + B_r e(t) & \text{if } e(t) \neq 0 \cup \tau \leq \rho \\ \tau^+ = 0,\ \mathbf{x}_r(t^+) = A_\rho \mathbf{x}_r(t) & \text{if } e(t) = 0 \cap \tau > \rho \\ u(t) = C_r\mathbf{x}_r(t) + D_r e(t) \end{cases} \tag{8}$$

where τ is a counter that starts counting after a reset and ρ is a tunable value that limits the time between resets.

2) Sinusoidal Input Describing Function: The SIDF describes the response of an element based purely on a sinusoidal input. For any SIDF to be correct there can be no missed resets. A standard reset system should reset twice per period, so the holding time cannot be longer than halve a period of the input sine without altering the response. Therefore the DF is only valid up to:

$$\omega_{DFmax} = \frac{\pi}{\rho} \tag{9}$$

3) Stability: Stability is sufficiently analyzed in [28].

B. Tuning rules

Consider a sinusoidal reference $r = A\sin(f2\pi t)$, based on linear control the error will be a sinusoid with $e = E\sin(f2\pi t + \phi)$ where ϕ is the phase shift. The error will cross zero twice per period, thus twice per period a reset should occur. The maximum reference the controller has to be able to track is the crossover frequency. Therefore the largest holding time cannot be bigger than halve a period at bandwidth (defined as crossover frequency):

$$\rho \leq \frac{1}{2f_c} \tag{10}$$

This will eliminate excessive resetting up to bandwidth and ensure the reliability of the DF in analysis.

Suppose that the crossover frequency varies due to gain variation, then holding time ρ might become to short for the new crossover frequency. Therefore a safety factor k has been included. An implementation of a safety factor k in the theory from Equation 10 results in Equation 11:

$$\rho = \frac{1}{2k \cdot f_c} \tag{11}$$

For shorthand the TR condition will be denoted as TR - $k \cdot f_c$.

C. Numerical sensitivity function

The same mass system as for Fig. 2 was taken in order to analyze the performance of the solution. Fig. 4 shows the performance increase achieved by implementing time regularization according to the tuning guideline with $k = \frac{5}{2}$. Where quantization has the worst influence for the standard reset condition an improvement of 10 dB is achieved.

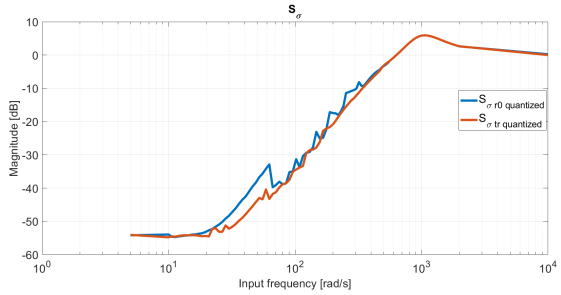

Fig. 4: S_σ with quantization for standard reset and TR - $\frac{5}{2} \cdot f_c$.

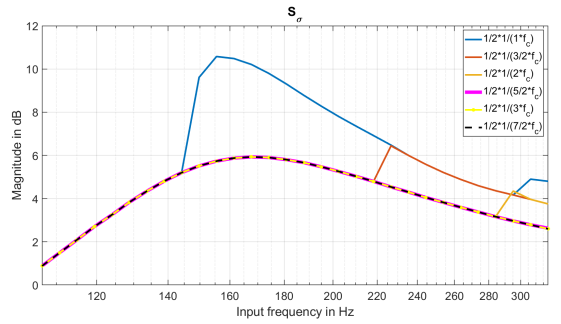

Fig. 5: The peak of S_σ for multiple values of ρ.

D. Sensitivity to ρ

In order to evaluate the tuning sensitivity with respect to ρ, S_σ was analyzed.

According to Equations 9 and 10 the holding time limits the describing function and performance up to a predetermined frequency. The peak of the sensitivity function is an important factor in control design. This peak is located at higher frequencies than the crossover frequency. This creates a trade off between lower frequency performance improvement and the high frequency sensitivity peak.

A long holding time will prevent more excessive resets than a shorter holding time, while also increasing the peak of the sensitivity function due to missed resets. Therefore an analysis in robustness and performance has been performed by implementing a range of safety factors k.

Especially the peak of S_σ and the frequency range where improvement is desired are analyzed. Fig. 5 shows the peak of S_σ for multiple values of ρ. It can be seen that ρ has a clear influence S_σ. ρ should be sufficiently low such that this peak is not increased. Especially the jump at 150 Hz for $\rho = \frac{1}{2f_c}$ clearly shows the result of resets being missed.

In Fig. 6 the influence of ρ on the frequency range of desired improvement is shown. The performance increases for shorter holding times, up to a limit. From Fig. 5 it can be seen that $\rho = \frac{1}{2} * \frac{1}{\frac{5}{2}f_c}$ is the shortest holding time without increasing the peak of sensitivity function. An increase in low frequency performance can be seen in Fig. 6. Due to its performance enhancement the following remark is made:

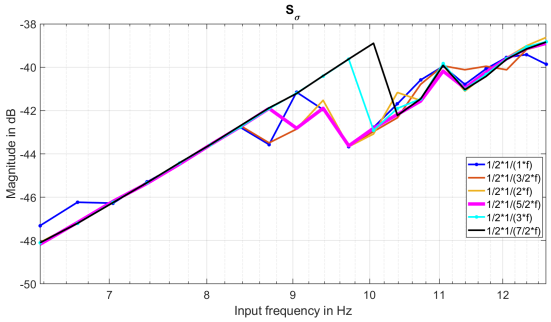

Fig. 6: The frequency range of desired improvement of S_σ for multiple values of ρ.

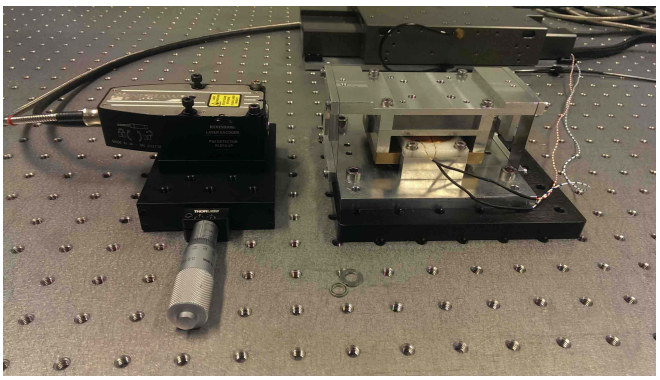

Fig. 7: Fine positioning stage.

Concluding from the sensitivity and performance analysis $k = \frac{5}{2}$ is the advised safety factor.

V. Application

A. Precision positioning stage

In order to validate the theory a custom designed one-degree-of-freedom high precision positioning stage has been used. In essence its a mass-spring system. The stage can be seen in Fig. 7. The sensor is a Renishaw RLE10 laser encoder set to 10 nm resolution per increment (inc.) and the actuator is Lorentz force based. In order to achieve fast real-time control an FPGA NI cRIO system was implemented with a sampling rate of 10 kHz.

Frequency response data of the system is obtained by applying chirp signals, as is common in industry. The results can be seen in Fig. 8. The following transfer function was found:

$$\frac{3.038e04}{s^2 + 0.7413s + 243.3}.$$

B. Designed controllers

It was decided to study CgLp-PID controller for a bandwidth, defined as crossover frequency, of 150 Hz and phase margin of 40°. The CgLp-PID was designed according to the transfer function of Equation 6 with the parameters shown in Table II. The controller was discretized according to the tustin

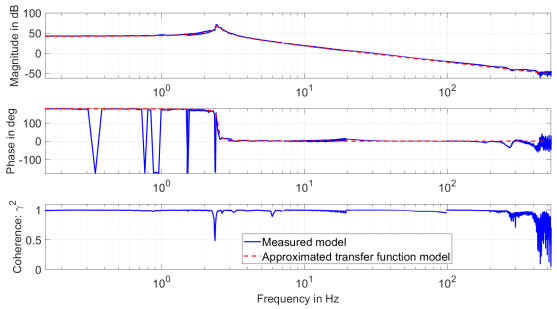

Fig. 8: Frequency response data and estimated model.

TABLE II: Controller settings for practical application.

P	16.41	-
γ	0	-
ω_c	942.5	rad/s
ω_i	94.25	rad/s
ω_d	529.2	rad/s
ω_t	1679	rad/s
$\omega_{r\alpha}$	697.6	rad/s
ω_r	812.1	rad/s
ω_f	9420	rad/s

method.

C. Results

In order to show that quantization induced performance degradation is not restricted to one specific Q, two Q's have been studied. The lowest 1 inc. resolution that corresponds to 10 nm and a numerical Q that shifted the resolution by 3 bits in order to achieve 8 inc. resolution.

1) 1 increment resolution: A reference amplitude of 3000 inc. (30μm) was applied at low frequencies. The minimum possible error is 1 inc. (10 nm), which leads to a limit of -69 dB. In practice this limit was not achieved due to noise and disturbance. Due to the limited linear stroke of the stage and saturation levels of the system the amplitude was decreased for higher frequencies.

For this quantization level in combination with the controller and plant dynamics the quantization induced performance degradation occurred at the lower frequency range. When regarding Fig. 9 a bump similar to Fig. 2 can be seen starting from 5 Hz and ending at 7.9 Hz. Time regularization based on $\rho = \frac{1}{f_c}$ shows a significant improvement for quantization induced performance degradation. In this case $\rho = \frac{1}{2}\frac{1}{147}$ due to the discrete nature of the program. As expected an increase in the sensitivity peak can be seen. Time regularization with $k = \frac{5}{2}$ shows an improvement in the low frequency domain while maintaining a proper peak in sensitivity function. Due to discretization, even the value of rho gets quantized in reality. This leads to an applied $\rho = \frac{1}{2}\frac{1}{385}$ of in this case.

2) 8 increment resolution: For the second quantization level of 80 nm again a reference amplitude of 3000 inc. (30μm) was applied for lower frequencies. The theoretical limit in this case is -51.5 dB. Here the theoretical and practical limit nicely agree because the noise level is small relative to the 80 nm resolution.

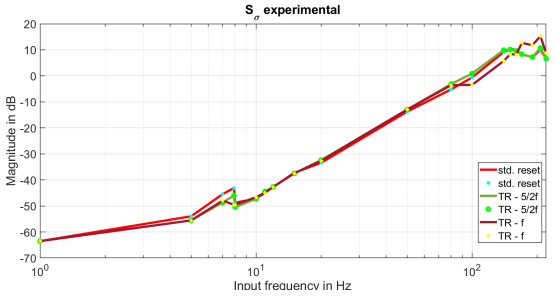

Fig. 9: Experimentally deduced sensitivity function for CgLp-PID with and without Time Regularization (TR - $\frac{5}{2} \cdot f_c$ and TR - f_c). For 10 nm resolution.

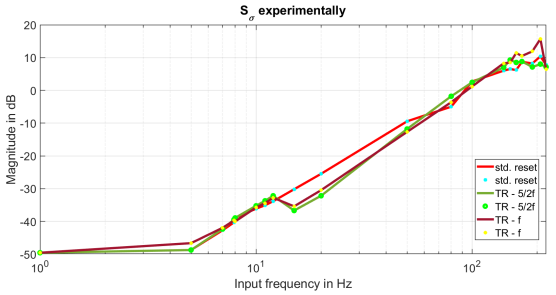

Fig. 10: Experimentally deduced sensitivity function for CgLp-PID with and without Time Regularization (TR - $\frac{5}{2} \cdot f_c$ and TR - f_c). For 80 nm resolution.

Fig. 10 shows the experimentally deduced sensitivity function. The quantization induced performance degradation was measured to be from 5 Hz up to 60 Hz. It can be seen that both TR show improvement, where TR - f_c shows the expected increased peak of sensitivity function.

3) Noise attenuation: Noise can increase the instances of excessive resetting. Time regularization influences the amount of resetting, therefore measurements have been performed to see the influence of time regularization. Fig. 11 shows the Cumulative Power Spectral Density (CPSD) of standard reset and time regularization. It can be seen that introducing a holding time can increase the noise attenuation.

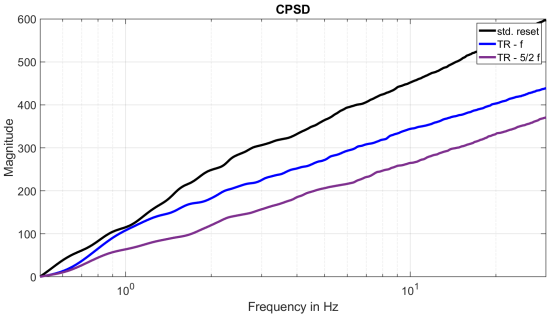

Fig. 11: Experimentally deduced Cumulative Power Spectral Density function for CgLp-PID with and without Time Regularization (TR - $\frac{5}{2} \cdot f_c$ and TR - f_c) for a maximum noise amplitude of 70 inc.

VI. Conclusion

The most common loop shaping method is PID, but it is limited by its linearity. Reset control is an addition to loop shaping and can overcome Bode's gain-phase relationship.

Reset control has been implemented in several practical applications, but no research has been done on the influence of quantization on performance. In this paper it is shown that quantization can reduce the performance of reset control elements.

Time regularization is implemented with a novel purpose. It is proposed as a solution for quantization induced performance degradation. Tuning guidelines are provided, with some robustness analysis.

The influence of time regularization on noise attenuation was experimentally measured to be beneficial.

Further research should be done in order to understand the effect of superposition on time regularized reset controllers.

Acknowledgment

The authors would like to thank Hittech Multin. This work was supported by NWO, through OTP TTW project #16335.

References

[1] H. W. Bode, *Network Analysis and Feedback Amplifier Design*. Princeton: van Nostrand New York.

[2] O. Beker, C. Hollot, and Y. Chait, "Plant With Integrator: An Example of Reset Control Overcoming Limitations of Linear Feedback," vol. 46, no. 11, pp. 1797–1799, 2001.

[3] J. C. Clegg, "A nonlinear integrator for servomechanisms," *Transactions of the American Institute of Electrical Engineers, Part II: Applications and Industry*, vol. 77, no. 1, pp. 41–42, 2013.

[4] I. Horowitz and P. Rosenbaum, "Non-linear design for cost of feedback reduction in systems with large parameter uncertainty," *International Journal of Control*, vol. 21, no. 6, pp. 977–1001, 1975.

[5] L. Hazeleger, M. Heertjes, and H. Nijmeijer, "Second-order reset elements for stage control design," *Proceedings of the American Control Conference*, vol. 2016-July, pp. 2643–2648, 2016.

[6] S. H. HosseinNia, I. Tejado, and B. M. Vinagre, "Fractional-order reset control: Application to a servomotor," *Mechatronics*, vol. 23, no. 7, pp. 781–788, oct 2013. [Online]. Available: https://linkinghub.elsevier.com/retrieve/pii/S0957415813000470

[7] A. Ba and A. Vidal, "Definition and tuning of a PI + CI reset controller," pp. 4792–4798, 2007.

[8] Y. Guo, Y. Wang, and L. Xie, "Frequency-domain properties of reset systems with application in hard-disk-drive systems," *IEEE Transactions on Control Systems Technology*, vol. 17, no. 6, pp. 1446–1453, 2009.

[9] N. Saikumar, R. K. Sinha, and S. H. HosseinNia, ""Constant in Gain Lead in Phase" Element– Application in Precision Motion Control," *IEEE/ASME Transactions on Mechatronics*, vol. 24, no. 3, pp. 1176–1185, jun 2019. [Online]. Available: https://ieeexplore.ieee.org/document/8681086/

[10] N. Saikumar, H. Hosseinnia, and M. Engineering, "Generalized Fractional Order Reset Element (GFrORE)," vol. 2, no. 1, 2017.

[11] A. Vidal and A. Baños, "Reset compensation for temperature control: Experimental application on heat exchangers," *Chemical Engineering Journal*, vol. 159, no. 1-3, pp. 170–181, 2010.

[12] H. Li, C. Du, and Y. Wang, "Optimal reset control for a dual-stage actuator system in HDDs," *IEEE/ASME Transactions on Mechatronics*, vol. 16, no. 3, pp. 480–488, 2011.

[13] H. Li, C. Du, Y. Wang, and Y. Guo, "Discrete-time optimal reset control for hard disk drive servo systems," *IEEE Transactions on Magnetics*, vol. 45, no. 11, pp. 5104–5107, 2009.

[14] Y. Zheng, Y. Chait, C. Hollot, M. Steinbuch, and M. Norg, "Experimental demonstration of reset control design," *Control Engineering Practice*, vol. 8, no. 2, pp. 113–120, feb 2000. [Online]. Available: https://linkinghub.elsevier.com/retrieve/pii/S0967066199001318

[15] F. S. Panni, H. Waschl, D. Alberer, and L. Zaccarian, "Position regulation of an EGR valve using reset control with adaptive feedforward," *IEEE Transactions on Control Systems Technology*, vol. 22, no. 6, pp. 2424–2431, 2014.

[16] A. Palanikumar, N. Saikumar, and S. H. Hosseinnia, "No More Differentiator in PID: Development of Nonlinear Lead for Precision Mechatronics," in *2018 European Control Conference, ECC 2018*. IEEE, jun 2018, pp. 991–996. [Online]. Available: https://ieeexplore.ieee.org/document/8550088/

[17] ——, "No More Differentiator in PID : Development of Nonlinear Lead for Precision Mechatronics."

[18] L. Chen, N. Saikumar, S. Baldi, and S. H. Hosseinnia, "Beyond the Waterbed Effect : Development of Fractional Order CRONE Control with Non-Linear Reset," 2019.

[19] "Quantization," in *Digital Video and HD*. Elsevier, 2012, pp. 37–46. [Online]. Available: https://linkinghub.elsevier.com/retrieve/pii/B9780123919267500047

[20] D. Rauth and V. Randal, "Analog-to-digital conversion. part 5," *IEEE Instrumentation & Measurement Magazine*, vol. 8, no. 4, pp. 44–54, oct 2005. [Online]. Available: http://ieeexplore.ieee.org/document/1634987/ http://ieeexplore.ieee.org/document/1518622/

[21] E. Lai, "Converting analog to digital signals and vice versa," *Practical Digital Signal Processing*, pp. 14–49, 2003.

[22] F. Ferrante, "On quantization and sporadic measurements in control systems: stability, stabilization, and observer design," *Dissertation*, 2015.

[23] F. Minyue, "Quantization for feedback control and estimation," *Proceedings of the 27th Chinese Control Conference, CCC*, pp. 751–756, 2008.

[24] J. H. Park, H. Shen, X. H. Chang, and T. H. Lee, "Quantized static output feedback control for discrete-time systems," *Studies in Systems, Decision and Control*, vol. 170, no. 8, pp. 41–67, 2019.

[25] J. Zheng and M. Fu, "A reset state estimator using an accelerometer for enhanced motion control with sensor quantization," *IEEE Transactions on Control Systems Technology*, vol. 18, no. 1, pp. 79–90, 2010.

[26] H. Zhu and H. Fujimoto, "Overcoming current quantization effects for precise current control using dithering techniques," *IEEJ Journal of Industry Applications*, vol. 2, no. 1, pp. 14–21, 2013.

[27] K. H. Johansson, M. Egerstedt, J. Lygeros, and S. Sastry, "On the regularization of Zeno hybrid automata," *Systems and Control Letters*, vol. 38, no. 3, pp. 141–150, 1999.

[28] D. Nešić, L. Zaccarian, and A. R. Teel, "Stability properties of reset systems," *Automatica*, vol. 44, no. 8, pp. 2019–2026, 2008.

[29] A. Baños and A. Barreiro, *Reset Control Systems*, ser. Advances in Industrial Control. London: Springer London, 2012. [Online]. Available: http://link.springer.com/10.1007/978-1-4471-2250-0

[30] C. Cai, A. A. Dastjerdi, N. Saikumar, and S. H. Hosseinnia, "The optimal sequence for reset controllers."

5

Preliminary analysis for combination of proposed solutions

5.1. Introduction

Two solutions to mitigate quantization induced performance deterioration have been proposed. These solutions work in different dimensions; a temporal dimension and a dimension that is shared with the reference amplitude. These two solutions can be combined, so the question arises whether they should be.

5.2. Preliminaries

5.2.1. Definition

The combination of the two aforementioned solutions can be defined as in Equation 5.1.

$$R_{\delta\rho}: \begin{cases} \dot{\tau} = 1, \dot{\mathbf{x}}_r(t) = A_r\mathbf{x}_r(t) + B_r e(t) & \text{if } (e(t), \dot{e}(t)) \notin B_\delta \cup \tau \leq \rho \\ \tau^+ = 0, \mathbf{x}_r(t^+) = A_\rho \mathbf{x}_r(t) & \text{if } (e(t), \dot{e}(t)) \in B_\delta \cap \tau > \rho \\ u(t) = C_r\mathbf{x}_r(t) + D_r e(t) & \end{cases} \tag{5.1}$$

where

$$\mathrm{B}_\delta = \{(x, y) \in \mathrm{R}^2 | (\mathrm{x} = -\delta \cap \mathrm{y} > 0) \cup (\mathrm{x} = \delta \cap \mathrm{y} < 0).$$

5.2.2. Sinusoidal Input Describing Function

For situations where the holding time is less than halve the period of the sinusoidal input the describing function of this combined solution should be identical to the DF of the reset band system, as shown in Chapter 3. So the DF of a reset band with time regularization is valid up to:

$$f_{DF\,max} = \frac{1}{2\rho}.$$

5.2.3. Stability

The system is stable under the conditions as stated in Chapter 3 and Chapter 4.

5.2.4. Tuning Rules

To analyze the tuning rules the same $\frac{1}{s^2}$ mass system as in Chapter 3 and Chapter 4 was analyzed with the CgLp-PID controller wit the values from Table 5.1 with 9 bits.

$$\underbrace{P(1+\frac{\omega_i}{s})}_{PI}\underbrace{\frac{(s/\omega_d+1)}{(s/\omega_t+1)}}_{D}\underbrace{\frac{1}{s/\omega_{r\alpha}+1}\gamma\frac{s/\omega_r+1}{s/\omega_f+1}}_{CgLp}$$

Figure 5.1 shows the sensitivity function (S_σ) as determined according to the formulation of [5] for a combination of reset band and time regularization. Implementing this combined solution with the original tuning

Table 5.1: Controller settings applied to the mass stage.

P	6.0954e+05	-
ω_c	942	rad/s
ω_i	94	rad/s
ω_d	530	rad/s
ω_t	1.68e+03	rad/s
$\omega_{r\alpha}$	160	rad/s
ω_f	9.42e+03	rad/s
ω_r	172	rad/s
γ	0.5	-
Range	5000	μ m
$f_{sampling}$	10	KHz
$T_{simulink}$	$1/(10f_{sampling})$	s

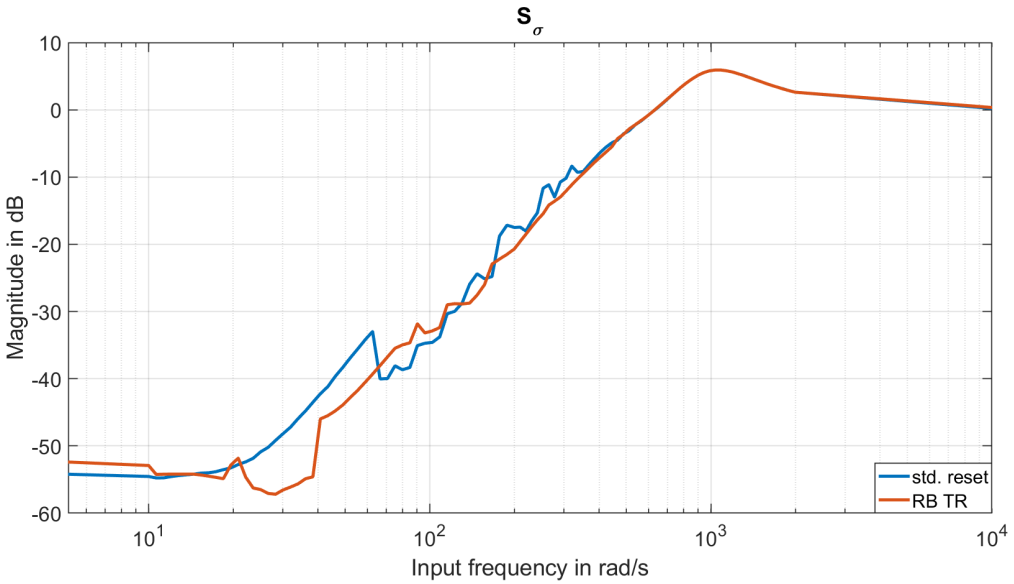

Figure 5.1: S_σ with quantization for reset band and time regularization combined, where RB TR signifies the combined solution.

rules, equation 5.2, results in the improvement for the low frequency domain ($\omega < 40$ rad/s) achieved by the applying the reset band. However, time regularization mitigates the degradation that applying the reset band normally induces. Therefore no bump can be seen.

$$\begin{aligned} |\delta| &> A \cdot |S|_{@f_{ref}} + \frac{Q}{2} \\ \rho &= \frac{1}{2k \cdot f_c}, \end{aligned} \tag{5.2}$$

where $k = \frac{5}{2}$.

5.3. Recommendation

It is recommended to do further research into the benefits and drawbacks of this combination of solutions. Especially a verification track with experimentation is required.

6

PID compared to CgLp-PID

As discussed before PID is limited by linearity in something that is described as either Bode's *Gain-Phase relationship* [4] or the *waterbed effect*. Reset elements can bypass these limitations. In literature it has been shown that reset control can outperform linear loop shaping methods, for example [3].

For an in depth analysis into CgLp- PID [21] is recommended. In this chapter experimental results related to the above papers will be discussed.

6.1. Precision positioning stage

The stage that was used for the experiments is a one-degree-of-freedom high precision positioning stage. It's essentially a mass-spring system. Fig. 6.1a shows a photograph of the stage. The sensor that was used is a Renishaw RLE10 laser encoder that was set to 10 nm increments (inc.). The actuator is a Lorentz force based actuator. For control an FPGA NI cRIO system was applied with a sampling rate of 10 kHz.

Frequency response data of the system is obtained by applying chirp signals, as is common in industry. The results can be seen in Fig. 6.1b. The following transfer function was found:

$$\frac{3.038e04}{s^2+0.7413s+243.3}.$$

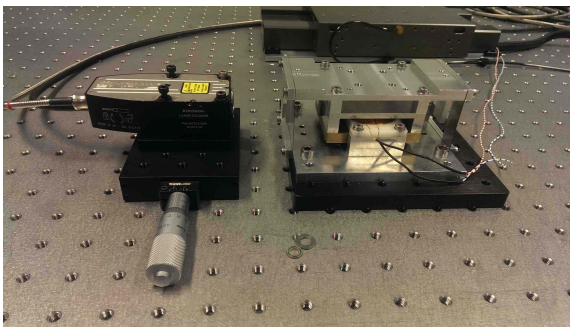

(a) Fine positioning stage.

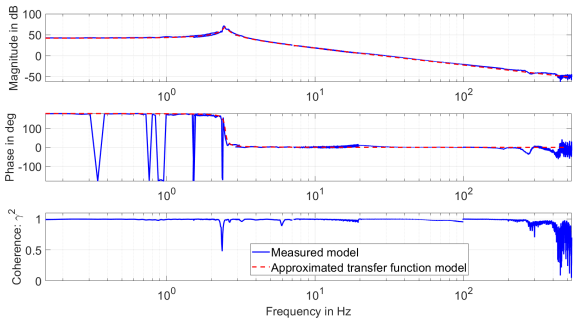

(b) Frequency response data and estimated model.

Figure 6.1: Physical and numerical model of the fine stage.

6.2. Designed controllers

It was decided to compare a linear PID·LPF controller with a CgLp-PID controller for a similar bandwidth of 150 Hz and phase margin of 40°. The PID·LPF is represented as:

$$\text{PID}\cdot\text{LPF} = P(1+\omega_i/s)\frac{(s/\omega_d+1)}{(s/\omega_t+1)}\frac{1}{\omega_f+1} \tag{6.1}$$

Table 6.1: Controller settings for practical application.

CgLp-PID			PID		
P	16.41	-	P	10.24	-
γ	0	-	-	-	-
ω_c	942.5	rad/s	ω_c	942.5	rad/s
ω_i	94.25	rad/s	ω_i	94.25	rad/s
ω_d	529.2	rad/s	ω_d	330.2	rad/s
ω_t	1679	rad/s	ω_t	2689	rad/s
$\omega_{r\alpha}$	697.6	rad/s	-	-	-
ω_r	812.1	rad/s	-	-	-
ω_f	9420	rad/s	ω_f	9425	rad/s

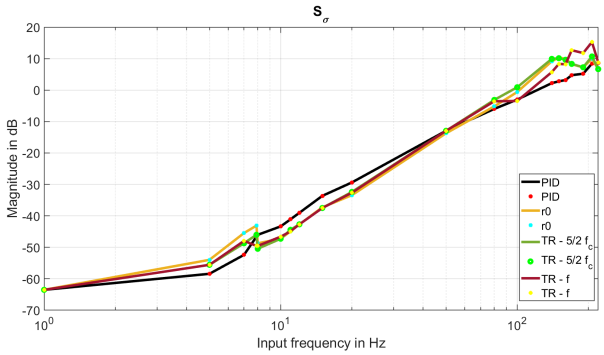

Figure 6.2: Sensitivity function based on experimental results for PID and various reset condition based CgLp-PID. 1 inc. resolution

Where $P(1+\omega_i/s)$=PI, $\frac{(s/\omega_d+1)}{(s/\omega_t+1)}$=D and $\frac{1}{s/\omega_f+1}$=LPF.
In order to get the required controller targets the values of Table 6.1 were applied.
A CgLp-PID can be represented as:

$$\text{CgLp-PID} = P(1+\omega_i/s)\frac{(s/\omega_d+1)}{(s/\omega_t+1)}\frac{1}{\cancel{s/\omega_{r\alpha}+1}}\frac{s/\omega_r+1}{\gamma s/\omega_f+1} \tag{6.2}$$

Where $\frac{1}{\cancel{s/\omega_{r\alpha}+1}}\frac{s/\omega_r+1}{\gamma s/\omega_f+1}$ = CgLp.
The corresponding CgLp-PID controller for a bandwidth of 150 Hz and phase margin of 40° is designed according to the variables in Table 6.1. It is important to note that the the order of elements was CgLp · PID.
The controllers were discretized according to the tustin method.

6.3. Results

Just like in the papers two quantization levels have been experimented with; 1 inc. (10nm) and 8 inc. (80 nm). In the following graphs the controllers are denoted as:

- Standard reset: r0;
- Time regularization with k: TR - $k \cdot f_c$;
- Reset band with δ: RBδ.

6.3.1. 1 increment resolution

Fig. 6.2 shows the sensitivity function based on experimental results. For this controller and system dynamics it was expected that PID would outperform CgLp-PID from about 70 Hz. However, it can be seen that PID CgLp-PID at lower frequencies as well. This is attributed to excessive resetting due to quantization. CgLp-PID outperforms PID at the mid-frequency range.

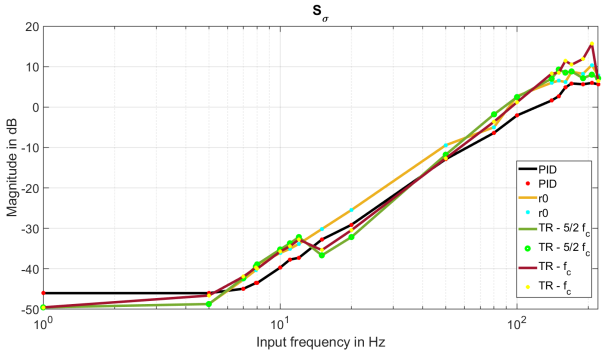

Figure 6.3: Sensitivity function based on experimental results for PID and various reset condition based CgLp-PID. 8 inc. resolution

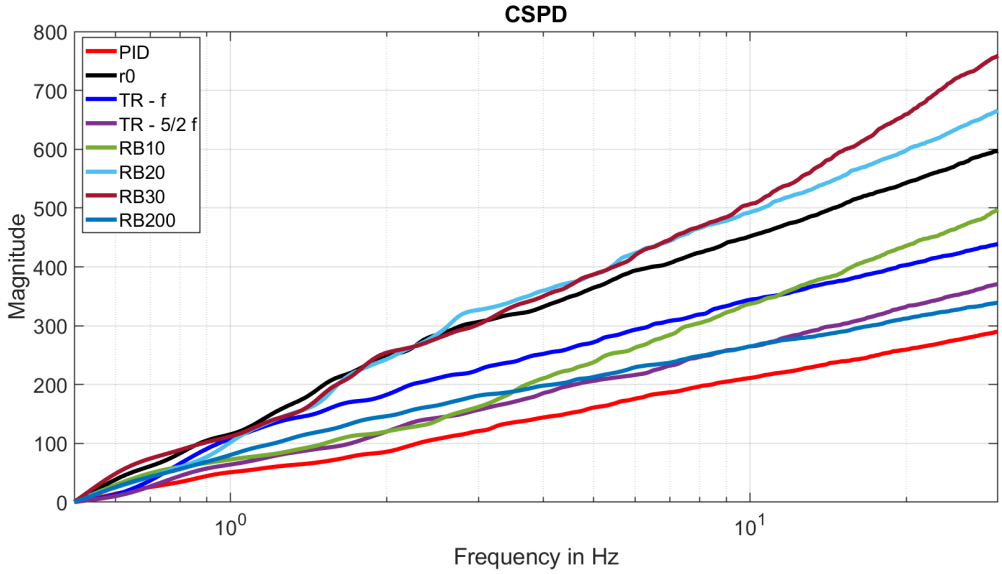

Figure 6.4: Cumulative Power Spectral Density (CPSD) for various controllers.

6.3.2. 8 increment resolution

When the resolution is decreased to 80 nm some interesting results are found. Fig. 6.3 shows the experimentally deduced sensitivity function. As before the PID is expected to outperform CgLp-PID at higher frequencies. Due to quantization the standard CgLp-PID is outperformed by PID in the mid-frequency range. However, when the time regularization solution is applied CgLp-PID will outperform PID.

6.3.3. Noise attenuation

Reset control is known to be able to attenuate noise better than linear PID [6, 16, 21]. This is attributed to the lowered dependency on the lead element, thus creating a lower slope at higher frequencies. However, noise can cause erroneous excessive resets thereby reducing noise attenuation. Fig. 6.4 shows the controllers noise attenuation abilities. It can be seen that PID outperforms the reset controllers for the designed controllers. Theory suggests that the reset controllers can be redesigned in order to increase the noise attenuation ability.

6.3.4. Disturbance rejection

The disturbance rejection of a setup can be analyzed in the frequency domain through a process sensitivity (PS) plot, where

$$PS = \frac{y}{d}.$$

Fig. 6.5 shows the process sensitivity that was experimentally deduced. The CgLp-PID is outperformed by the PID for most of the frequency range. However, when time regularization is applied the performance of reset control is better than linear PID. TR - f_c has an increased PS for higher frequencies due to the missing resets

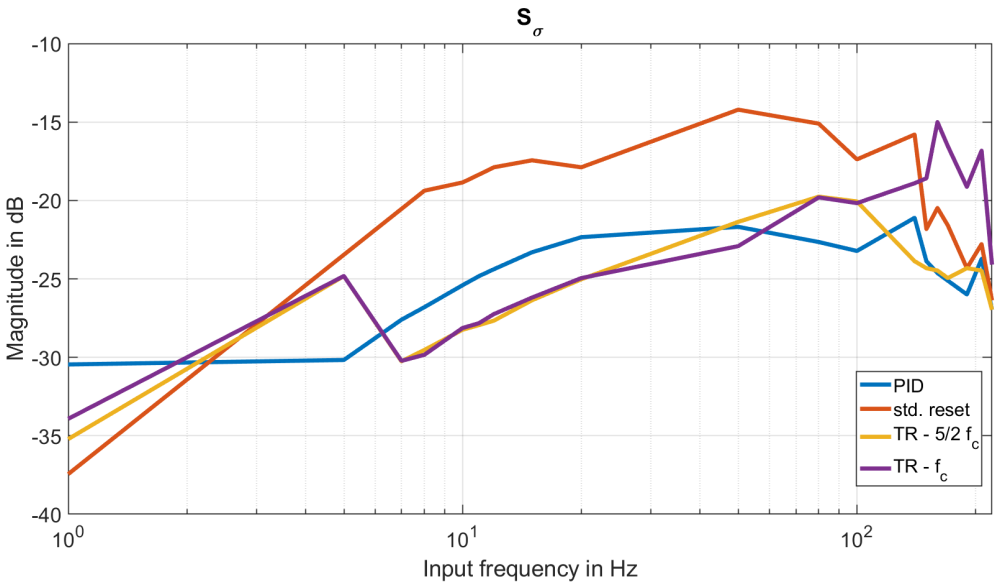

Figure 6.5: Process sensitivity function for various controllers.

that occur because of long holding time ρ.

7

Conclusion

7.1. General conclusions

In this thesis reset band and time regularization have been implemented in reset control, CgLp-PID specifically, in order to reduce the performance degradation that is caused by quantization. Tuning guidelines for both reset band and time regularization have been provided.

Numerical simulations in Matlab Simulink have been performed in order to analyze the dynamics of quantization induced performance degradation. Based on the understanding of these dynamics two solutions have been proposed: reset band and time regularization. Tuning guidelines for both solutions have been researched. A robustness analysis is performed in order to show the sensitivity to the tuning rules.

Experiments were conducted to show the practical performance of both proposed solutions. These were performed on a custom high resolution positioning stage that was controlled by an FPGA NI cRIO unit that controlled a Lorentz force based actuator and got feedback from a Renishaw RLE10 laser encoder.

The results of implementing a reset band show that for the frequency it is tuned for the performance can be increased significantly. In some recorded cases the error over reference magnitude was improved by 6 dB. However, as expected it can deteriorate performance when the frequency is increased. Depending on the magnitude of the reset band, noise attenuation can either be improved or degraded. When inspecting the Cumulative Power Spectral Density (CSPD) a maximum improvement of a magnitude of 200 was recorded. However, with an especially detrimental value for the reset band a deterioration of magnitude 200 was recorded.

Time regularization is a more global and robust solution in the frequency domain. It has been shown to improve or equal performance over the entire relevant frequency domain. Where quantization induced performance degradation was worst an improvement of 3 dB was recorded. Moreover, noise attenuation was shown to have improved as well as disturbance rejection. For noise attenuation the altered controller that followed the tuning rules showed a maximum improvement in CSPD of a magnitude of 200. For disturbance an improvement of 10 dB in output over disturbance was not uncommon.

Reset band as a solution against quantization can have the drawback that it is tuned for specific input frequencies, and disturbance and noise levels. In high-tech system these variables are often well known and can thus be taken into account.

Time regularization is shown to be more robust and forgiving. If properly tuned it works well for the entire frequency range. This is because of to the superior sensitivity to the tunable parameter ρ versus the tunable parameter of the reset band (δ).

It has been shown that quantization can cause performance degradation that can be countered by implementing a reset band or time regularization.

7.2. Recommendations

The two paper chapters (Chapter 3 and Chapter 4) have focused on reset control. There it was shown that the solutions can improve performance. However, in Chapter 6 the research was put into perspective with a PID

baseline. In this case it can be seen that the reset controller that was used did not perform optimally. It has been shown that reset control can outperform PID more than that was the case here. It would be interesting to analyze the effect of reset band and time regularization on various different controllers, of which multiple CgLp-PID and multiple different reset elements.

7.2.1. Reset band

For the reset band solution it would be interesting to design an adaptive reference guided reset band magnitude. This could be based on input through a Fourier analysis in combination with the sensitivity function. Another possibility is to monitor excessive resetting and tune the reset band width accordingly. Another possibility is the application of a variable / advanced reset band.

It would also be interesting to experimentally deduce a sensitivity function. For this a stage with a large linear stroke is required, where saturation cannot cause an issue. In other words the entire frequency range needs to be analyzed for a single reference amplitude.

The application of an observer can decrease the required value of δ.

7.2.2. Time regularization

For time regularization it is interesting to analyze the performance under superposition. Moreover, time regularization can be combined with an adaptive realtime "fixed" time reset method.

7.2.3. Combination of reset band and time regularization

Some preliminary results suggest that both methods can be combined without negatively affecting each other. Time regularization seems to mitigate the shifted degradation from the application of a reset band. However, more research needs to be done in this field. Numerical, analytical and experimental information is required to be able to determine the viability of combining reset band with time regularization.

7.2.4. Other

Several other paths of research have been rejected due to the conflict of time constraints versus potential. Some of these can be interesting to research if alternatives for reset band of time regularization are desired.

A linear Low Pass Filter (LPF) can be added in the reset condition loop. LPF has the effect of spreading out the energy of incoming signals. Thus the quantization levels will be less hard. The drawback of this system is that an LPF introduces additional phase lag. Moreover the distortion frequency is related to several variables which can change. Therefore a single corner frequency might not suffice.

A related solution is the application of an observer. This can diminish distortion while also possibly introducing phase loss. Non-linear observers have been applied in order to mitigate quantization distortion.

A (moving) notch filter. If it were possible to place a notch filter exactly on the distortion frequency this might result in the filtering out of distortion. Once again the difficulty lies in the knowing of the distortion frequency. For a constant ramp, quantization level and system dynamics, this would be constant However, for a sine with a changing slope the frequency will change over the period.

A linearization of distortion could level out the spikes. This could be attempted with the use of a predicted slope based on a derivative. However, a common problem with derivatives is something that is known as a "Derivative kick". This results in a very steep slope that can occur because the sampling is such that there is a sample just before and just after a quantization level transition. That being said, if the sampling for the derivative is done correctly a derivative kick caused by quantization could be avoided. Although noise can still be amplified.

The same method for slope prediction could be applied in order to estimate the distortion frequency for the next time samples. Essentially a form of predictor or estimator could be designed.

Bibliography

[1] Alfonso Baños and Antonio Barreiro. *Reset Control Systems*. Advances in Industrial Control. Springer London, London, 2012. ISBN 978-1-4471-2216-6. doi: 10.1007/978-1-4471-2250-0. URL http://link.springer.com/10.1007/978-1-4471-2250-0.

[2] Antonio Barreiro, Alfonso Banos, and Sebastian Dormido. Reset Control Systems with Reset Band: Well-posedness and Limit Cycles Analysis. In *2011 19th Mediterranean Conference on Control & Automation (MED)*, pages 1343–1348. IEEE, jun 2011. ISBN 978-1-4577-0124-5. doi: 10.1109/MED.2011.5983109. URL http://ieeexplore.ieee.org/document/5983109/.

[3] Orhan Beker, C.V. Hollot, and Y. Chait. Plant With Integrator: An Example of Reset Control Overcoming Limitations of Linear Feedback. 46(11):1797–1799, 2001.

[4] Hendrik W Bode. *Network Analysis and Feedback Amplifier Design*. van Nostrand New York, Princeton.

[5] Chengwei Cai, A A Dastjerdi, Niranjan Saikumar, and S Hassan Hosseinnia. The optimal sequence for reset controllers.

[6] Linda Chen, Niranjan Saikumar, Simone Baldi, and S Hassan Hosseinnia. Beyond the Waterbed Effect : Development of Fractional Order CRONE Control with Non-Linear Reset. 2019.

[7] J. C. Clegg. A nonlinear integrator for servomechanisms. *Transactions of the American Institute of Electrical Engineers, Part II: Applications and Industry*, 77(1):41–42, 2013. ISSN 0097-2185. doi: 10.1109/tai.1958.6367399.

[8] George Ellis. *Control System Design Guide*. 2012. ISBN 9780123859204. doi: 10.1016/C2010-0-65994-3.

[9] Yuqian Guo, Yuoyi Wang, and Lihua Xie. Frequency-domain properties of reset systems with application in hard-disk-drive systems. *IEEE Transactions on Control Systems Technology*, 17(6):1446–1453, 2009. ISSN 10636536. doi: 10.1109/TCST.2008.2009066.

[10] Leroy Hazeleger, Marcel Heertjes, and Henk Nijmeijer. Second-order reset elements for stage control design. *Proceedings of the American Control Conference*, 2016-July:2643–2648, 2016. ISSN 07431619. doi: 10.1109/ACC.2016.7525315.

[11] Isaac Horowitz and Patrick Rosenbaum. Non-linear design for cost of feedback reduction in systems with large parameter uncertainty. *International Journal of Control*, 21(6):977–1001, 1975. ISSN 13665820. doi: 10.1080/00207177508922051.

[12] S. Hassan HosseinNia, Inés Tejado, and Blas M Vinagre. Fractional-order reset control: Application to a servomotor. *Mechatronics*, 23(7):781–788, oct 2013. ISSN 09574158. doi: 10.1016/j.mechatronics.2013.03.005. URL https://linkinghub.elsevier.com/retrieve/pii/S0957415813000470.

[13] Monkol Konghirun, Xu Longya, and Jennifer Skinner-Gray. Quantization Errors in Digital Control Systems.

[14] Hui Li, Chunling Du, Youyi Wang, and Yuqian Guo. Discrete-time optimal reset control for hard disk drive servo systems. *IEEE Transactions on Magnetics*, 45(11):5104–5107, 2009. ISSN 00189464. doi: 10.1109/TMAG.2009.2029629.

[15] Hui Li, Chunling Du, and Youyi Wang. Optimal reset control for a dual-stage actuator system in HDDs. *IEEE/ASME Transactions on Mechatronics*, 16(3):480–488, 2011. ISSN 10834435. doi: 10.1109/TMECH.2011.2123104.

[16] Arun Palanikumar, Niranjan Saikumar, and S Hassan Hosseinnia. No More Differentiator in PID : Development of Nonlinear Lead for Precision Mechatronics.

[17] Francesco Saverio Panni, Harald Waschl, Daniel Alberer, and Luca Zaccarian. Position regulation of an EGR valve using reset control with adaptive feedforward. *IEEE Transactions on Control Systems Technology*, 22(6):2424–2431, 2014. ISSN 10636536. doi: 10.1109/TCST.2014.2308915.

[18] Christophe Prieur, Isabelle Queinnec, Sophie Tarbouriech, and Luca Zaccarian. *Analysis and synthesis of reset control systems*. PhD thesis, 2018.

[19] D.A. Rauth and V.T. Randal. Analog-to-digital conversion. part 5. *IEEE Instrumentation & Measurement Magazine*, 8(4):44–54, oct 2005. ISSN 1094-6969. doi: 10.1109/MIM.2005.1518622. URL http://ieeexplore.ieee.org/document/1634987/http://ieeexplore.ieee.org/document/1518622/.

[20] Niranjan Saikumar, S Hassan Hosseinnia, and Erdi Akyüz. Reset Control for Vibration Isolation.

[21] Niranjan Saikumar, Rahul Kumar Sinha, and S. Hassan HosseinNia. "Constant in Gain Lead in Phase" Element– Application in Precision Motion Control. *IEEE/ASME Transactions on Mechatronics*, 24(3):1176–1185, jun 2019. ISSN 1083-4435. doi: 10.1109/TMECH.2019.2909082. URL https://ieeexplore.ieee.org/document/8681086/.

[22] Robert Munnig Schmidt, Georg Schitter, and Jan van Eijk. *The design of high performance mechatronics*. 2011. ISBN 9781607508250.

[23] Angel Vidal and Alfonso Baños. Reset compensation for temperature control: Experimental application on heat exchangers. *Chemical Engineering Journal*, 159(1-3):170–181, 2010. ISSN 13858947. doi: 10.1016/j.cej.2010.02.033.

[24] Jinchuan Zheng and Minyue Fu. A reset state estimator using an accelerometer for enhanced motion control with sensor quantization. *IEEE Transactions on Control Systems Technology*, 18(1):79–90, 2010. ISSN 10636536. doi: 10.1109/TCST.2009.2014467.

[25] Y. Zheng, Y. Chait, C.V. Hollot, M. Steinbuch, and M. Norg. Experimental demonstration of reset control design. *Control Engineering Practice*, 8(2):113–120, feb 2000. ISSN 09670661. doi: 10.1016/S0967-0661(99)00131-8. URL https://linkinghub.elsevier.com/retrieve/pii/S0967066199001318.

[26] Hongzhong Zhu and Hiroshi Fujimoto. Overcoming current quantization effects for precise current control using dithering techniques. *IEEJ Journal of Industry Applications*, 2(1):14–21, 2013. ISSN 21871108. doi: 10.1541/ieejjia.2.14.